Inorganic Chemistry

ARTICLE

pubs.acs.org/IC

# Unusual Ligand Transformations Initiated by dppm Deprotonation in Methylene-Bridged Rh/Os Complexes

Kyle D. Wells, Robert McDonald,[†] Michael J. Ferguson,[†] and Martin Cowie*

Department of Chemistry, University of Alberta, Edmonton, Alberta, Canada T6G 2G2; [†]X-ray Crystallography Laboratory.

Supporting Information

**ABSTRACT:** The reaction of $[RhOs(CO)_3(\mu\text{-}CH_2)(dppm)_2][CF_3SO_3]$ (dppm = $\mu$-$Ph_2PCH_2PPh_2$) with 1,3,4,5-tetramethylimidazol-2-ylidene ($IMe_4$) results in competing substitution of the Rh-bound carbonyl by $IMe_4$ and dppm deprotonation by $IMe_4$ to give the two products $[RhOs(IMe_4)(CO)_2(\mu\text{-}CH_2)(dppm)_2][CF_3SO_3]$ and $[RhOs(CO)_3(\mu\text{-}CH_2)(\mu\text{-}\kappa^1\text{:}\eta^2\text{-dppm-H})(dppm)]$ [**3**; dppm-H = bis(diphenylphosphino)methanide], respectively. In the latter product, the dppm-H group is P-bound to Os while bound to Rh by the other $PPh_2$ group and the adjacent methanide C. The reaction of the tetracarbonyl species $[RhOs(CO)_4(\mu\text{-}CH_2)(dppm)_2][CF_3SO_3]$ with $IMe_4$ results in the exclusive deprotonation of a dppm ligand to give $[RhOs(CO)_4(\mu\text{-}CH_2)(\mu\text{-}\kappa^1\text{:}\kappa^1\text{-dppm-H})(dppm)]$ (**4**) in which dppm-H is P-bound to both metals. Both deprotonated products are cleanly prepared by the reaction of their respective precursors with potassium bis(trimethylsilyl)amide. Reversible conversion of the $\mu$-$\kappa^1$:$\eta^2$-dppm-H complex to the $\mu$-$\kappa^1$:$\kappa^1$-dppm-H complex is achieved by the addition or removal of CO, respectively. In the absence of CO, compound **3** slowly converts in solution to $[RhOs(CO)_3(\mu\text{-}\kappa^1\text{:}\kappa^1\text{:}\kappa^1\text{-}Ph_2PCHPPh_2CH_2)(dppm)]$ (**5**) as a result of dissociation of the Rh-bound $PPh_2$ moiety of the dppm-H group and its attack at the bridging $CH_2$ group. Compound **4** is also unstable, yielding the ketenyl- and ketenylidene/hydride tautomers $[RhOs(CO)_3(\mu\text{-}\kappa^1\text{:}\eta^2\text{-CHCO})(dppm)_2]$ (**6a**) and $[RhOs(H)(CO)_3(\mu\text{-}\kappa^1\text{:}\kappa^1\text{-CCO})(dppm)_2]$ (**6b**), initiated by proton transfer from $\mu$-$CH_2$ to dppm-H. Slow conversion of these tautomers to a pair of isomers of $[RhOs(H)(CO)_3(\mu\text{-}\kappa^1\text{:}\kappa^1\text{:}\kappa^1\text{-}Ph_2PCH(COCH)PPh_2)(dppm)]$ (**7a** and **7b**) subsequently occurs in which proton transfer from a dppm group to the ketenylidene fragment gives rise to coupling of the resulting dppm-H methanide C and the ketenyl unit. Attempts to couple the ketenyl- or ketenylidene-bridged fragments in **6a**/**6b** with dimethyl acetylenedicarboxylate (DMAD) yield $[RhOs(\kappa^1\text{-CHCO})(CO)_3(\mu\text{-DMAD})(dppm)_2]$, in which the ketenyl group is terminally bound to Os.

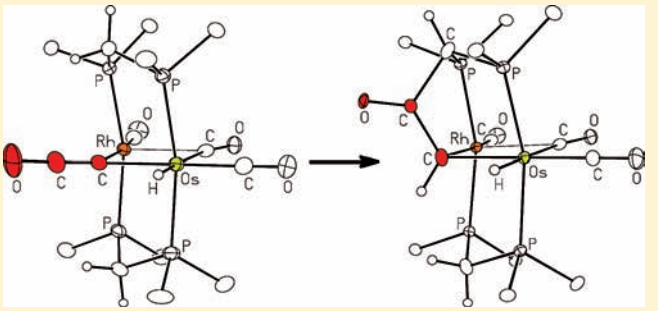

## INTRODUCTION

In an earlier study,[1a] in which we had attempted to synthesize methylene-bridged complexes, incorporating the N-heterocyclic carbene (NHC) ligand 1,3,4,5-tetramethylimidazol-2-ylidene ($IMe_4$), by the reaction of $[RhOs(CO)_3(\mu\text{-}CH_2)(dppm)_2][CF_3SO_3]$ (dppm = $\mu$-$Ph_2PCH_2PPh_2$) with $IMe_4$, we observed dual Lewis and Brønsted−Lowry basicity of this carbene through the competitive formation of a targeted methylene-bridged species, $[RhOs(IMe_4)(CO)_2(\mu\text{-}CH_2)(dppm)_2][CF_3SO_3]$, together with an unexpected product of dppm deprotonation, $[RhOs(CO)_3(\mu\text{-}CH_2)(\mu\text{-}\kappa^1\text{:}\eta^2\text{-dppm-H})(dppm)]$ (**3**; dppm-H = bis(diphenylphosphino)methanide), as outlined in Scheme 1. Deprotonation of the acidic methylene protons of dppm is not particularly unusual,[2,3] and NHC groups are known to be Brønsted bases;[4] nevertheless, such acid−base chemistry is not the "conventional" reactivity observed for NHC ligands in late-metal complexes, in which they more typically behave as "phosphine mimics" binding effectively to the metals.[5,6]

This dichotomic behavior of $IMe_4$ has recently been observed by us in a number of closely related complexes of Rh/Os, in which deprotonation of either acetonitrile, methyl, or dppm ligands had occurred under some conditions, while conventional coordination of $IMe_4$ to Rh had occurred under others.[1] We were therefore interested in determining the conditions under which $IMe_4$ would function as a conventional ligand and under which its Brønsted basicity would predominate.

We were also interested in studying the reactivity of these dppm-H groups. Sharp and co-workers had observed an

**Scheme 1**

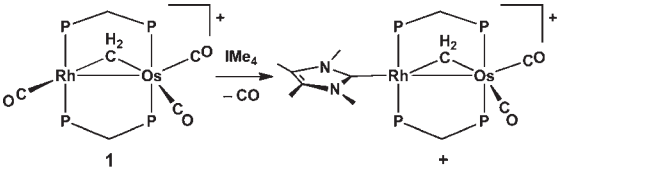


**Received:** December 9, 2010
**Published:** March 11, 2011

  

**Chart 1**

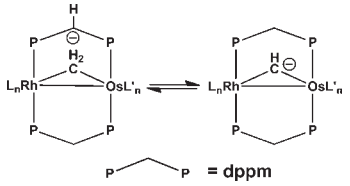


interesting conversion of amido-bridged/dppm-H species to the imido-bridged/dppm tautomers by reversible proton transfer from the amido group to dppm-H.[3] On the basis of these observations, we considered the possibility of analogous proton transfer between a bridging methylene group and dppm-H, as outlined in Chart 1, to generate a methylidyne-bridged product; such anionic methylidyne groups should be highly nucleophilic and should display interesting reactivity.

In our earlier report,[1a] which concentrated on the reactivity of the $IMe_4$-containing, methylene-bridged product, shown in Scheme 1, we did not discuss the characterization and subsequent chemistry of compound **3**, which now forms the main focus of the current paper.

## EXPERIMENTAL SECTION

**General Comments.** All solvents were dried using the appropriate desiccants, distilled before use, and stored under nitrogen. Reactions were performed under an argon atmosphere using standard Schlenk techniques. The 1,3,4,5-tetramethylimidazol-2-ylidene ($IMe_4$) ligand was prepared using a published procedure[7] and then recrystallized from toluene to afford colorless crystals, which were stored at −30 °C. For reactions that did not require its isolation, a standardized solution containing $IMe_4$ in tetrahydrofuran (THF; 0.2133 M) was used; this solution was stored over potassium in the freezer and used without further purification. Dimethyl acetylenedicarboxylate (DMAD), Diazald, Diazald-*N*-methyl-$^{13}C$ and Diazald-*N*-methyl-$d_3$ were purchased from Aldrich and were used without further purification, while potassium bis(trimethylsilyl)amide was obtained from the same source and handled under inert conditions. Carbon monoxide was purchased from Praxair, and $^{13}CO$ (99.5%) was obtained from Cambridge Isotope Laboratories. The compounds $[RhOs(CO)_3(\mu\text{-}CH_2)(dppm)_2][CF_3SO_3]$ (**1**), $[RhOs(CO)_4(\mu\text{-}CH_2)(dppm)_2][CF_3SO_3]$ (**2**), and their $^{13}CH_2$- and $CD_2$-labeled analogues were prepared using published procedures by using the appropriately labeled Diazald to generate the labeled species.[8]

NMR spectra were recorded using a Varian iNova-400 spectrometer operating at 399.8 MHz for $^1H$, 161.8 MHz for $^{31}P$, and 100.6 MHz for $^{13}C$ nuclei. IR spectra were obtained on solutions using a Nicolet Magna 760 spectrometer or on solid samples using a NicPlan FTIR spectrometer. Elemental analyses were performed by the microanalytical service within the department using a CE 1108 CHNS-O analyzer. Electrospray ionization mass spectra were acquired on a Micromass ZabSpec spectrometer by the staff in the departmental mass spectrometry facility. In all cases, the distribution of isotope peaks matched the calculated isotopic distribution for the appropriate parent ion very closely. Spectroscopic data for all compounds are given in Table 1.

**Preparation of Compounds.** *a. $[RhOs(CO)_3(\mu\text{-}CH_2)(Ph_2PCHPPh_2)(dppm)]$ (**3**).* **Method i**: To a deep-red solution containing **1** (300 mg, 0.23 mmol) in 10 mL of THF at ambient temperature was added 1.1 equiv of $IMe_4$ (1.2 mL, 0.213 M THF) dropwise via a syringe, turning the solution yellow. A purge needle was inserted into the solution, and a gentle argon purge was employed during stirring for 1 h. An aliquot of the reaction mixture showed a 4:1 ratio of the desired product **3** and $[RhOs(IMe_4)(CO)_2(\mu\text{-}CH_2)(dppm)_2][CF_3SO_3]$,[1a] respectively, as determined by $^{31}P$ NMR spectroscopy. The $IMe_4$-containing product and $[HIMe_4][OTf]$ were precipitated as a dark-red oil by the addition of 10 mL of pentane to the reaction mixture. The resulting bright-yellow supernatant containing **3** was separated from the oil and evaporated to dryness in vacuo (yield 62%). **Method ii**: To a red solution consisting of **1** (98 mg, 0.076 mmol) dissolved in 5 mL of THF at ambient temperature was added, via a cannula, 1 equiv of $KN(Si(CH_3)_3)_2$ (15 mg, 0.076 mmol) dissolved in 2.5 mL of THF, giving a bright-yellow solution, which was allowed to stir for 30 min. A 10 mL portion of pentane was added to give an off-white precipitate, determined to be potassium triflate. This precipitate was separated from the mother liquor by filtering through Celite. The remaining pale-yellow solution was evaporated to dryness, in vacuo, and then washed with 2 × 5 mL portions of pentane to give a bright-yellow solid (85 mg, 84%). **Method iii**: To a slurry containing **2** (200 mg, 0.15 mmol) in 10 mL of THF was inserted a needle, through which a steady stream of argon was passed into the mixture. An equimolar amount of $IMe_4$ (0.70 mL, 0.2133 M in THF) was delivered to the reaction flask dropwise to give a light-orange solution. The solution was stirred for 1 h under an argon purge, a 5 mL portion of pentane was added to fully precipitate the insoluble byproduct, and the resulting mixture was filtered through a bed of Celite. The mother liquor was removed in vacuo, giving a yellow solid (yield 92%). This crude product was dissolved in a minimum volume of $Et_2O$ (approximately 5 mL) and then precipitated upon the addition of 15 mL of pentane. The bright-yellow solid was separated from the pale-yellow supernatant and dried further in vacuo (yield 85%). Anal. Calcd for $C_{54}H_{45}O_3P_4RhOs$: C, 55.96; H, 3.91. Found: C, 55.95; H, 4.13. The $^{31}P\{^1H\}$, $^{13}C\{^1H\}$, and $^1H$ NMR spectra for **3** are provided in the Supporting Information. **Method iv**: To a slurry containing **2** (200 mg, 0.152 mmol) in 5 mL of THF at ambient temperature was inserted a needle, through which a steady stream of argon was passed into the mixture. A total of 1 equiv of $KN(Si(CH_3)_3)_2$ (30 mg, 0.152 mmol) dissolved in 2.5 mL of THF was added via a cannula to the slurry, giving a bright-yellow solution, which was allowed to stir for 30 min. A 10 mL portion of pentane was added to give an off-white precipitate, determined to be potassium triflate. This was separated from the mother liquor by filtering through Celite. The remaining pale-yellow solution was evaporated to dryness, in vacuo, an then washed with 2 × 5 mL portions of pentane to give a bright-yellow solid (85 mg, 84%).

*b. NMR Investigations of $[RhOs(CO)_4(\mu\text{-}CH_2)(Ph_2PCHPPh_2)(dppm)]$ (**4**).* **Method i**: To a 20 mg portion of $^{13}CO$-labeled compound **3**, dissolved in 0.7 mL of THF-$d^8$ at ambient temperature, was added 1.5 mL of $^{13}CO$ via a gastight syringe. The solution gradually turned dark orange, and **4** was observed via $^{31}P$ NMR spectroscopy. This species could not be isolated, leading instead to the formation of compound **3** via $^{13}CO$ loss. Attempts to generate **4** at low temperature by the reaction of **3** with CO failed, with no reaction observed until near ambient temperature. However, generating **4** at ambient temperature, as described above, and then cooling to −80 °C after 5 min allowed the observation of **4** and **3** in a 1:2 ratio, while inhibiting the transformation of **4** into subsequent products. Owing to its instability, compound **4** was characterized at −80 °C by NMR spectroscopy. **Method ii**: Monitoring the reactions discussed in part a, methods iii and iv, in sealed NMR tubes via $^{31}P$ NMR spectroscopy showed **4** to be the sole product initially present in a THF-$d^6$ solution upon the addition of base to **2**. Monitoring these reactions for 1 h via $^{31}P$ NMR demonstrated the conversion of **4** to **3**.

*c. $[RhOs(CO)_3(Ph_2PCHPPh_2CH_2)(dppm)]$ (**5**).* **Method i**: A bright-yellow solution containing 150 mg (0.13 mmol) of **3** in 5 mL of THF was refluxed gently under an argon gas atmosphere for 1 h, after which time a $^{31}P\{^1H\}$ NMR spectrum of a reaction-mixture aliquot indicated quantative conversion to compound **5**. The solvent was removed in vacuo and the residue washed with 2 × 5 mL of pentane before drying under reduced pressure to yield 125 mg (83%). **Method ii**: The quantitative transformation from **3** to **5** could also be carried out by leaving **3** in a THF solution at ambient temperature for 2 days. Crystals used for elemental analysis were obtained by diffusion of pentane into a concentrated THF solution of **5**. Anal. Calcd from crystals giving the

**Table 1. Spectroscopic Data for the Compounds**

| | | NMR[a] | | |
|---|---|---|---|---|
| compound | IR ($cm^{-1}$)[b] | $\delta(^{31}P\{^1H\})$[c] | $\delta(^1H)$[d,e] | $\delta(^{13}C\{^1H\})$[d,e] |
| $[RhOs(CO)_3(\mu\text{-}CH_2)$-(dppm-H)(dppm)] (**3**) | 1974 (s), 1956 (s), 1893 (s) | $P_A$, 48.5 (dddd); $P_B$, 6.5 (dd, dppm); $P_C$, −3.2 (ddd); $P_D$, −7.2 (dddd, dppm-H)[f] $J$ (Hz): $P_AP_B$ = 89, $P_AP_C$ = 18, $P_AP_D$ = 2, $P_BP_D$ = 282, $P_CP_D$ = 21, $P_ARh$ = 143, $P_CRh$ = 87, $P_DRh$ = 11 | 5.18 (dm, 1H, $^2J_{HH}$ = 6.0 Hz, $^1J_{CH}$ = 134.5 Hz), 4.45 (dm, 1H, $^2J_{HH}$ = 6.0 Hz, $^1J_{CH}$ = 140.8 Hz, $\mu$-$CH_2$), 4.62 (ddd, 1H, $^2J_{HH}$ = 14 Hz, $^2J_{HP}$ = 23.4 Hz), 3.47 (bdd, 1H, $^2J_{HH}$ = 14.0 Hz, $^2J_{HP}$ = 23.9 Hz, dppm), 1.38 (m, 1H, $^2J_{HRh}$ = 1.6 Hz, dppm-H)[f] | 188.2 (dm, 1C, $^1J_{CRh}$ = 65 Hz, Rh−CO), 188.1 (dd, 1C, $^2J_{CP(Os)}$ = 8, 8 Hz), 186.1 (dd, 1C, $^2J_{CP(Os)}$ = 7, 7 Hz, Os−CO), 75.0 (m, 1C, $\mu$-$CH_2$, $^1J_{CRh}$ = 21 Hz), 40.0 (dd, 1C, $^1J_{CP}$ = 25, 25 Hz, dppm) |
| $[RhOs(CO)_4(\mu\text{-}CH_2)$-(dppm-H)(dppm)] (**4**) | NA | $P_C$, 45.4 (dddd); $P_D$, 2.1 (ddd, dppm-H); $P_A$, 24.3 (dddd); $P_B$, −7.0 (ddd, dppm)[f,g] $J$ (Hz): $P_CP_A$ = 253, $P_CP_D$ = 125, $P_CP_B$ = 16, $P_DP_A$ = 21, $P_DP_B$ = 226, $P_AP_B$ = 89, $P_CRh$ = 149, $P_ARh$ = 143 | 4.08, 3.32 (ddd, 1H, $^2J_{HH}$ = 14.0 Hz, $^2J_{HP}$ = 11.0, 11.0 Hz, dppm), 2.24, 2.20 (dm, 1H, $^2J_{HH}$ = 5.7 Hz, $\mu$-$CH_2$), 0.44 (br m, 1H, dppm-H)[f,g] | 215.0 (dd, 1C, $^1J_{CRh}$ = 32 Hz, $^2J_{CC}$ = 16 Hz, $\mu$-CO), 200.1 (dd, 1C, $^1J_{CRh}$ = 59 Hz, $^2J_{CC}$ = 24 Hz, Rh−CO), 182.1 (m, 1C, $^2J_{CC}$ = 16 Hz), 181.4 (m, 1C, $^2J_{CC}$ = 7.5 Hz, Os−CO), 35.7 (br m, 1C, $\mu$-$CH_2$)[f,g] |
| $[RhOs(CO)_3(Ph_2PCHP$-$Ph_2CH_2)$(dppm)] (**5**) | 1949 (s), 1924 (s), 1889 (s) | $P_A$, 29.1 (dddd); $P_B$, −2.2 (ddd, dppm); $P_C$, 12.4 (dddd); $P_D$, 0.2 (dddd, $Ph_2PCHPPh_2CH_2$)[i] $J$ (Hz): $P_AP_C$ = 14, $P_AP_D$ = 6, $P_AP_B$= 77, $P_CP_D$ = 70, $P_CP_B$ = 14, $P_BP_D$ = 255, $P_ARh$ = 165, $P_CRh$ = 6, $P_DRh$ = 6 | 5.29 (dddd, 1H, $^3J_{HRh}$ = 3.0 Hz, $^2J_{HH}$ = 15.2 Hz, $^2J_{HP(A)}$ = 8.0 Hz, $^2J_{HP(B)}$ = 10.0 Hz), 4.57 (ddd, 1H, $^2J_{HH}$ = 15.2 Hz, $^2J_{HP(A)}$ = 11.0 Hz, $^2J_{HP(B)}$ = 9 Hz, dppm), 4.19 (dm, 1H, $^2J_{HRh}$ = 1.9 Hz, CH), 1.84 (br dddd, 1H, $^2J_{HH}$ = 13.6 Hz, $^2J_{HP(C)}$ = 8 Hz, $^3J_{HP(B)}$ = $^3J_{HP(D)}$ = 2 Hz), 1.64 (br dddd, 1H, $^2J_{HH}$ = 13.6 Hz, $^2J_{HP(C)}$ = 14.0 Hz, $^3J_{HP(D)}$ = $^3J_{HP(B)}$ = 13.0 Hz, $CH_2$, $Ph_2PCHPPh_2CH_2$)[i] | 188.7 (dd, 1C, $^1J_{CRh}$ = 72 Hz, $^2J_{CP(Rh)}$ = 11 Hz, Rh−CO), 190.0 (dd, 1C, $^2J_{CP(Os)}$ = 9 Hz, $^2J_{CC}$ = 13 Hz, Os−CO), 186.2 (m, 1C, Os−CO), 60.6 (dd, 1C, $^1J_{CP}$ = 21 Hz, 31 Hz, dppm), 1.5 (m, 1C, CH), −22.6 (dddd, $^1J_{CP}$ = 45 Hz, $^2J_{CP}$ = 5, 5 Hz, $^2J_{CC}$ = 13 Hz, $CH_2$, $Ph_2PCHPPh_2CH_2$)[i] |
| $[RhOs(CO)_3(\mu\text{-}CHCO)$-$(dppm)_2]$ (**6a**) | 1964 (br s), 1775 (s) | 13.8 (dm, $^1J_{PRh}$ = 142 Hz), −0.2 (m, dppm)[i] −80 °C: $\delta$ 21.0, 9.3, 2.0, 0.9 | 4.57, 4.08 (dm, 2H, $^2J_{HH}$ =14.5 Hz, dppm), 4.28 (dttd, 1H, $^1J_{CH}$ = 169 Hz, $^3J_{HP(Os)}$ = 8.4 Hz, $^3J_{HP(Rh)}$ = 4.9 Hz, $^{2,3}J_{HRh}$ = 3.6 Hz, $\mu$-CHCO)[i] | 191.3 (dt, 1C, $^1J_{CRh}$ = 69 Hz, $^2J_{CP}$ = 14 Hz, Rh−CO), 193.1 (dt, 1C, $^2J_{CP}$ = 9 Hz, $^2J_{CC}$ = 13 Hz), 182.5 (br t, 1C, $^2J_{CP}$ = 8 Hz, Os−CO), 214.6 (dddt, $^1J_{CC}$ = 52 Hz, $^2J_{CP}$ = 11 Hz, $^1J_{CRh}$ = 9 Hz, $J_{CH}$ = 7 Hz, CO), 22.0 (ddd, 1C, $^1J_{CH}$ = 169 Hz, $^1J_{CC}$ = 52 Hz, $^2J_{CC}$ = 13 Hz, $^2J_{CRh}$ = 7 Hz, CH, $\mu$-CHCO)[i] |
| $[RhOs(H)(CO)_3(\mu\text{-}CCO)$-$(dppm)_2]$ (**6b**) | 2011 (s), 1953 (s), 1932 (s), 1904 (s) | 26.3 (dm, $^1J_{PRh}$ = 144 Hz), −3.6 (m, dppm)[i] | 4.35 (dddd, 2H, $^2J_{HH}$ = 13.5 Hz, $^2J_{HP}$ = $^3J_{HRh}$ = 6.0 Hz), 2.71 (dm, 2H, $^2J_{HH}$ = 13.5, dppm), −7.01 (dtt, 1H, $^3J_{HP(Os)}$ = 20.9 Hz, $^3J_{HP(Rh)}$ = 2.5 Hz, $^2J_{HC}$ = 17 Hz, Os−H)[i] | 195.4 (ddt, 1C, $^1J_{CRh}$ = 69 Hz, $^2J_{CC}$ = 22 Hz, $^2J_{CPRh}$ = 15 Hz, Rh−CO), 186.6 (br d, 1C, $^2J_{CH}$ = 17 Hz, Os−CO), 182.2 (t, 1C, $^2J_{CP}$ = 7 Hz, $^2J_{CC}$ = 15 Hz, $^2J_{CH}$ = 8 Hz, Os−CO), 160.6 (d, 1C, $^1J_{CC}$ = 112 Hz), −5.5 (dm, $^1J_{CC}$ = 112 Hz, $^2J_{CC}$ = 22, 15 Hz, $^1J_{CRh}$ = 22 Hz, $\mu$-C, $\mu$-CCO)[i] |



dx.doi.org/10.1021/ic102470j |*Inorg. Chem.* 2011, 50, 3523–3538

**Table 1. Continued**

| compound | IR ($cm^{-1}$)[b] | NMR[a] $\delta(^{31}P\{^1H\})$[c] | NMR[a] $\delta(^1H)$[d,e] | NMR[a] $\delta(^{13}C\{^1H\})$[d,e] |
|---|---|---|---|---|
| [RhOs(H)(CO)$_3$-($\mu$-$Ph_2PCH(COCH)PPh_2$)-(dppm)] (**7a**) | 2017 (s), 1957 (s), 1798 (s), 1587 (m) | $P_A$, 35.2 (dddd); $P_B$, 4.8 (dddd); $P_C$, −9.2 (dddd); $P_D$, −28.9 (dddd)[i] $J$ (Hz): $P_AP_B$ = 80, $P_AP_C$ = 303, $P_AP_D$ = 19, $P_BP_C$ = 9, $P_BP_D$ = 249, $P_CP_D$ = 26, $P_ARh$ = 154, $P_BRh$ = 4, $P_CRh$ = 138, $P_DRh$ = 2 | 4.16 (ddd, 1H, $^3J_{HC}$ = 8 Hz, $^2J_{HP}$ = $^2J_{HP}$ = 8 Hz, dppm-H), 4.10 (br dddm, 1H, $^1J_{HC}$ = 142 Hz, $^2J_{HP}$ = 20 Hz, $^3J_{HH}$ = 1.5 Hz, CH), 3.24 (ddd, 1H, $^2J_{HH}$ = 14.1 Hz, $^2J_{HP}$ = $^2J_{HP}$ = 11 Hz), 2.74 (ddd, 1H, $^2J_{HH}$ = 14.1 Hz, $^2J_{HP}$ = $^2J_{HP}$ = 10 Hz, dppm), −7.58 (ddddd, 1H, $^2J_{HP}$ = $^2J_{HP}$ = 20 Hz, $^4J_{HP}$ = 5 Hz, $^3J_{HRh}$ = 4 Hz, $^3J_{HH}$ = 1.5 Hz, Os−H)[i] | 200.3 (dddd, 1C, $^1J_{CRh}$ = 63 Hz, $^2J_{CP}$ = 16 Hz, $^2J_{CC}$ = 17 Hz, Rh−CO), 197.2 (br m, 1C, $^2J_{CH}$ = 15 Hz, $^1J_{CRh}$ = 3 Hz, $^2J_{CP}$ = unresolved, Os−CO), 183.8 (br ddd, 1C, $^2J_{CP}$ = $^2J_{CP}$ = 8 Hz, $^2J_{CC}$ = 11 Hz, $^3J_{CH}$ = 8 Hz, Os−CO), 210.9 (ddddd, 1C, $^1J_{CC}$ = 49 Hz, $^3J_{CP}$ = 16, 16, 16, 16 Hz, CO), 66.8 (br dm, $^1J_{CC}$ = 49 Hz, $^1J_{CH}$ = 145 Hz, $^1J_{CRh}$ = $^1J_{CC}$ = 16 Hz, $^1J_{CC}$ = 11 Hz, CH)[i] |
| [$RhOs(CO)_3$($\mu$-H)($\mu$-$Ph_2PCH(COCH)PPh_2$)-(dppm)] (**7b**) | 2006 (s), 1938 (s), 1918 (s) 1568 (m) | $P_A$, 38.3 (dddd); $P_B$, 8.7 (ddd); $P_C$, −8.6 (dddd); $P_D$, −26.2 (ddd); dppm[i] $J$ (Hz): $P_AP_B$ = 95, $P_AP_C$ = 255, $P_AP_D$ = 21, $P_BP_C$ = 6, $P_BP_D$ = 261, $P_CP_D$ = 29, $P_ARh$ = 175,$P_BRh$ = 2, $P_CRh$ = 154, $P_DRh$ = 2 | 4.05 (br dddd, 1H, $^2J_{HRh}$ = $^2J_{HP}$ = 1.9 Hz, $^2J_{HP}$ = 7.3 Hz, $^2J_{HC}$ = 8.0 Hz, dppm-H), 3.73 (dddtd, 1H,$^1J_{HC}$ = 139.0 Hz, $^3J_{HP}$ = 20.1, 4.7, 4.7 Hz, $^3J_{HH}$ = 2.5 Hz, CH), 2.80 (ddd, 1H, $^2J_{HH}$ = 14.3 Hz, $^2J_{HP}$ = 9.6 Hz), 2.61 (br dm, 1H, $^2J_{HH}$ = 14.3 Hz, dppm), −7.45 (ddddd, $^1J_{HRh}$ = 17.1 Hz, $^2J_{HP}$ = 9 Hz, $^3J_{HH}$ = 2.5 Hz, $\mu$-H)[i] | 205.3 (dddd, 1C, $^1J_{CRh}$ = 61 Hz, $^2J_{CC}$ = $^2J_{CP}$ = $^2J_{CP}$ =16 Hz, Rh−CO), 185.1 (ddd, 1C, $^2J_{CP}$ = $^2J_{CC}$ = 8 Hz, OsCO), 179.8 (ddd, 1C, $^2J_{CP}$ = 4 Hz, $J_{CH}$ = 12 Hz Os−CO), 213.6 (br ddddd, 1C, $^1J_{CC}$ = 43 Hz, $^3J_{CP}$ = 20, 13, 6, 4.5 Hz, $C_6O$), 66.8 (m, $^1J_{CC}$ = 43 Hz, $^1J_{CH}$ = 139 Hz, CH)[i] |
| [RhOs(CHCO)$(CO)_3$($\mu$-DMAD)$(dppm)_2$] (**9**) | 2026, 1971, 1925, 1882, 1688 (1676 sh) | 20.4 (dm, $^1J_{PRh}$ = 157 Hz), −6.8 (m, dppm)[h] | 4.59, 2.96 (dm, 2H, $^2J_{HH}$ = 14.5 Hz), 0.59 (dt, 1H, $^3J_{HP(Os)}$ = 3.6 Hz, $^1J_{CH}$ = 165.2 Hz), 3.27, 1.72 (s, 3H, DMAD)[h] | 194.2 (dt, 1C, $^1J_{CRh}$ = 59 Hz, $^2J_{CP}$ = 12 Hz, Rh−CO), 195.2 (ddt, 1C, $^2J_{CC}$ = 21 Hz, $^1J_{CRh}$ = $^2J_{CP(Os)}$ = 9 Hz, $\mu$-CO), 183.4 (br t, 1C, $^2J_{CP}$ = 7 Hz, Os−CO), 180.8 (dt, $^1J_{CC}$ = 96 Hz, $^3J_{CPOs}$ = 2 Hz, CO), −19.1 (dddt, 1C, $^1J_{CH}$ = 165 Hz, $^2J_{CC}$ = 96, 21 Hz, $^2J_{CP}$ = 7 Hz, CH), 183.7 (tt, 1C, $^2J_{CP}$ = 11 Hz), 155.2 (dtt, 1C, $^1J_{CRh}$ = 21 Hz, $^2J_{CP}$ = 6 Hz, C≡C), 177.6 (br dt, 1C, $^2J_{CRh}$ =$^3J_{CP}$ = 2 Hz), 165.3 (t, 1C, $^3J_{CP}$ = 2 Hz. CO), 49.3, 48.8, (s, 1C, DMAD)[h] |

[a] NMR abbreviations: s = singlet, d = doublet, t = triplet, m = multiplet, br = broad. NMR data at 298 K unless otherwise indicated. [b] IR abbreviations: s = strong, m = medium, br = broad, sh = shoulder. [c] $^{31}P$ chemical shifts referenced to external 85% $H_3PO_4$. [d] Chemical shifts for the phenyl hydrogens and carbons not given. [e] $^1H$ and $^{13}C$ chemical shifts referenced to TMS. [f] $C_4D_8O$. [g] −80 °C. [h] $CD_2Cl_2$. [i] $C_6D_6$.



dx.doi.org/10.1021/ic102470j |*Inorg. Chem.* 2011, 50, 3523–3538

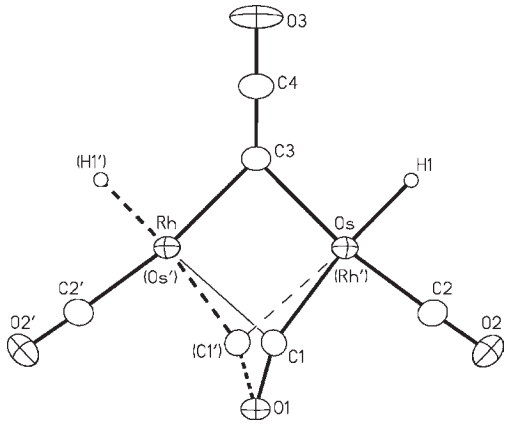


**Figure 1.** View within the equatorial plane of **6b** showing the disorder of the Rh, Os, C1, and H1 atoms. The dppm groups above and below the equatorial plane are omitted for clarity.

formulation $C_{59}H_{57}O_3OsP_4Rh$ (**5**·$C_5H_{12}$): C, 57.56; H, 4.67. Found: C, 57.22; H, 4.55. The presence of 1 equiv of pentane was confirmed by $^1$H NMR spectroscopy in $CD_2Cl_2$.

*d. [RhOs(CO)$_3$(μ-CHCO)(dppm)$_2$] (**6a**) + [RhOs(H)(CO)$_3$(μ-CCO)-(dppm)$_2$] (**6b**).* A stirred solution containing compound **3** (250 mg, 0.22 mmol), dissolved in 5 mL of benzene, was gently purged with CO gas for 30 min, during which time the color gradually turned from yellow to bright orange. Upon complete conversion of **3** to the observed 1:1 mixture of **6a** and **6b** (30 min, as confirmed by $^{31}$P NMR spectroscopy), the solution was concentrated to approximately 1 mL in vacuo and left overnight to give orange crystals that were determined by single-crystal X-ray crystallography to consist only of **6b** (223 mg, 87%). The crystals were separated from the mother liquor, which contained the impurity [RhOs(CO)$_4$(dppm)$_2$][OAc], which had resulted from the reaction of the target species with adventitious water. Dissolution of the crystals of **6b** in $C_6D_6$ produced a 1:1 ratio of **6a**/**6b**. Anal. Calcd for $C_{55}H_{45}O_4P_4RhOsC_9D_9$ (**6b**·1.5$C_6D_6$): C, 58.54; H, 4.83. Found: C, 58.55; H, 4.42. $^{31}$P{$^1$H}, $^{13}$C{$^1$H}, and $^1$H NMR spectra for compounds **6a**/**6b** are provided in the Supporting Information.

*e. Reaction of **6a**/**6b** with CO and $H_2O$.* Under a CO atmosphere, 3 μL of $H_2O$ (4 equiv, 0.17 mmol) was added to a solution containing **6a** and **6b** (50 mg, 0.042 mmol) in 0.7 mL of $C_6D_6$. The NMR spectra ($^{31}$P, $^{13}$C, and $^1$H) of the final product, [RhOs(CO)$_4$(dppm)$_2$][OAc], were essentially identical with those previously reported for [RhOs(CO)$_4$(dppm)$_2$][BF$_4$],[9] while the acetate counterion was identified by $^{13}$C NMR [δ 21.0 (dq, $^1J_{CH}$ = 131 Hz, $^1J_{CC}$ = 61), 169.2 (dq, $^2J_{CH}$ = 7 Hz, $^1J_{CC}$ = 61)] and $^1$H NMR spectroscopy [δ 2.15 ($^1J_{CH}$ = 131 Hz, $^2J_{CH}$ = 7 Hz)].

*f. [RhOs(H)(CO)$_3$(μ-Ph$_2$PCH(COCH)PPh$_2$)(dppm)] (**7a**).* A solution containing the 1:1 mixture of **6a** and **6b** (50 mg, 0.042 mmol) in 0.7 mL of THF-$d^8$, maintained at ambient temperature for 7 days, cleanly generated **7a** as the sole product, as determined by $^{31}$P NMR spectroscopy. This transformation occurred within 3 h in refluxing THF and within 30 min in refluxing benzene; however, at these temperatures, subsequent transformation to **7b** also began to occur (see procedure g). A yellow solid was isolated from the ambient-temperature reaction upon removal of the solvent in vacuo, and this solid was rinsed with 2 × 0.5 mL of pentane and dried further in vacuo (48 mg, 96%). Anal. Calcd for $C_{55}H_{45}O_4P_4RhOs$: C, 55.65; H, 3.82. Found: C, 55.92; H, 4.02.

*g. [RhOs(CO)$_3$(μ-H)(μ-Ph$_2$PCH(COCH)PPh$_2$)(dppm)] (**7b**).* Heating a solution containing **7a** (50 mg, 0.042 mmol) in 0.7 mL of $C_6D_6$ to 80 °C generated **7b** in approximately 30 min in quantitative yield, as determined by $^{31}$P NMR spectroscopy. Slow evaporation in benzene afforded a crystalline material, which was separated from the mother liquor and dried in vacuo. Anal. Calcd for $C_{55}H_{45}O_4P_4RhOs$: C, 55.65; H, 3.82. Found: C, 55.72; H, 3.92.

*h. [RhOs(CHCO)(CO)$_3$(μ-DMAD)(dppm)$_2$] (**8**).* To a solution containing a mixture of **6a** and **6b** (100 mg, 0.084 mmol) in 5 mL of THF was added 11 μL of DMAD (0.090 mmol, 1.05 equiv), resulting in a color change from orange to dark red. After stirring for 4 h, the solvent was reduced to approximately 1 mL, and 10 mL of pentane was added to precipitate an orange solid, which was separated and dried further in vacuo (yield 94%). Anal. Calcd for $C_{61}H_{51}O_8P_4RhOs$: C, 55.12; H, 3.87. Found: C, 54.76; H, 3.85. Compound **8** underwent partial hydrolysis by adventitious water to give [RhOs(CO)$_3$(μ-DMAD)(dppm)$_2$][OAc], which has NMR features essentially identical with those of the known species, [RhOs(CO)$_3$(μ-DMAD)(dppm)$_2$][BF$_4$].[9] Quantitative conversion to [RhOs(CO)$_3$(μ-DMAD)(dppm)$_2$][OAc] was achieved by the addition of 1 equiv of $H_2O$.

**X-ray Data Collection and Structure Solution.** *a. General Procedures.* Data sets for **3** and **5** were collected using a Bruker SMART 1000 CCD detector/PLATFORM diffractometer[10] using Mo Kα radiation, with the crystals cooled to −80 °C. Data sets for compounds **6b** and **7a** were collected using a Bruker APEX II CCD detector/D8 diffractometer[10] using Mo Kα radiation, with the crystals cooled to −100 °C. The data were corrected for absorption through use of the *SADABS*[10] multiscan model (**3** and **5**) or the numerical integration model (**6b** and **7a**). Structures were solved by Patterson search/structure expansion (*DIRDIF-99*[11] for **3** or *DIRDIF-2008*[12] for **6b**) or by direct methods/structure expansion (*SIR97* for **5** and **7a**).[13] Refinements were completed using the program *SHELXL-97*.[14] Nonhydridic H atoms were assigned positions based on the idealized sp$^2$ or sp$^3$ geometries of their attached C atoms and were given thermal parameters 20% greater than those of the attached C atoms. See the Supporting Information for a listing of the crystallographic experimental data.

*b. Crystal Growth and Special Refinement Conditions.* (i) Yellow crystals of compound **3** were grown via diffusion of *n*-pentane into a THF solution of the compound. Distances within the disordered solvent THF molecule were given fixed idealized values during refinement: *d*(O20S−C21S) = *d*(O20S−C24S) = *d*(O30S−C31S) = *d*(O30S−C34S) = 1.46(1) Å; *d*(C21S−C22S) = *d*(C22S−C23S) = *d*(C23S−C24S) = *d*(C31S−C32S) = *d*(C32S−C33S) = *d*(C33S−C34S) = 1.52(1) Å; *d*(O20S···C22S) = *d*(O20S···C23S) = *d*(O30S···C32S) = *d*(O30S···C33S) = 2.43(1) Å; *d*(C21S···C23S) = *d*(C22S···C24S) = *d*(C31S···C33S) = *d*(C32S···C34S) = 2.55(1) Å; *d*(C21S···C24S) = *d*(C31S···C34S) = 2.36(1) Å. (ii) Yellow crystals of compound **5** were grown via diffusion of *n*-pentane into a dichloromethane solution of the compound. Distance restraints were applied to the disordered solvent *n*-pentane molecules: C−C bond distance = 1.53(1) Å, 1,3-C···C distance = 2.50(1) Å, *d*(C1SB···C5SB) = 2.90(1) Å. One dppm phenyl group was modeled as disordered, with both orientations of this phenyl ring constrained to be idealized hexagons with C−C distances of 1.39 Å. (iii) Orange crystals of **6b** were grown from a concentrated solution containing tautomers **6a** and **6b** in benzene. Compound **6b** was found to be disordered across the crystallographic mirror plane (*x*, *y*, 0). An illustration of the disorder mode of the metals, the semibridging carbonyl, and the hydride ligand is shown in Figure 1, in which the dppm ligands above and below the plane of the drawing are unaffected by the disorder and have been omitted. Solid bonds connect the atoms of one disordered molecule, while heavy dashed lines connect the disordered atoms of the other. The metal atom positions are modeled as a combination of 50% Os/50% Rh sharing the same sites, while the C1 and H1 atoms are equally disordered across the mirror plane. Note that none of the other atoms within the complex are affected by the disorder; these atoms either are lying on the mirror plane or are related to an identical group by the mirror plane. One carbonyl C atom (C1) was located at a position slightly offset from the mirror plane and refined with an occupancy factor of 50%. The hydrido ligand was input in a position

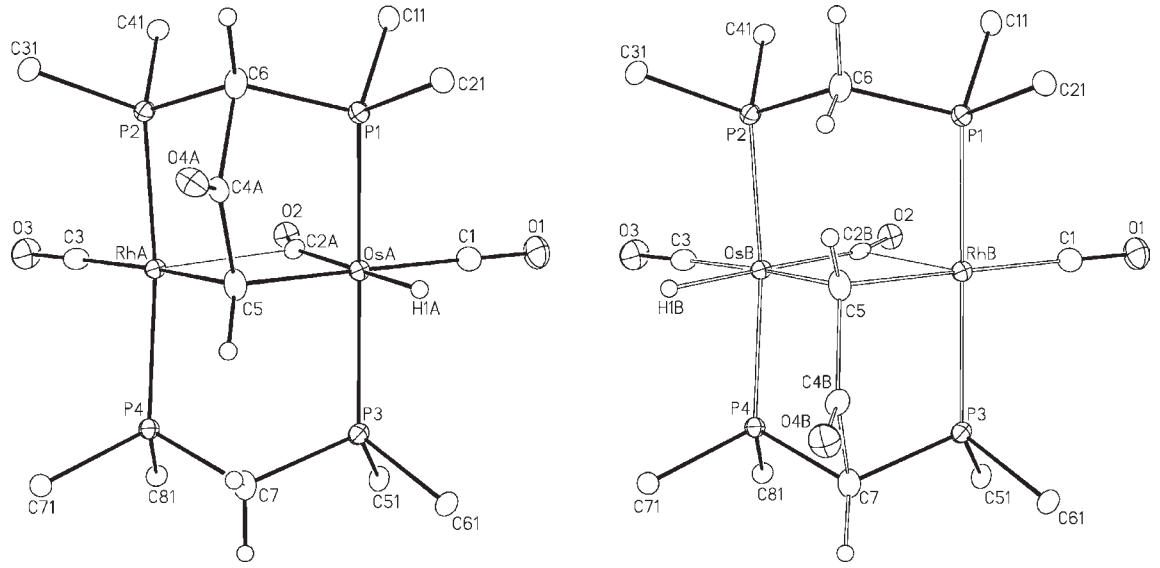


**Figure 2.** Molecule A (left) and molecule B (right) of **7a** showing the disorder described. Only the *ipso*-C atoms of the dppm phenyl groups are shown.

**Scheme 2**

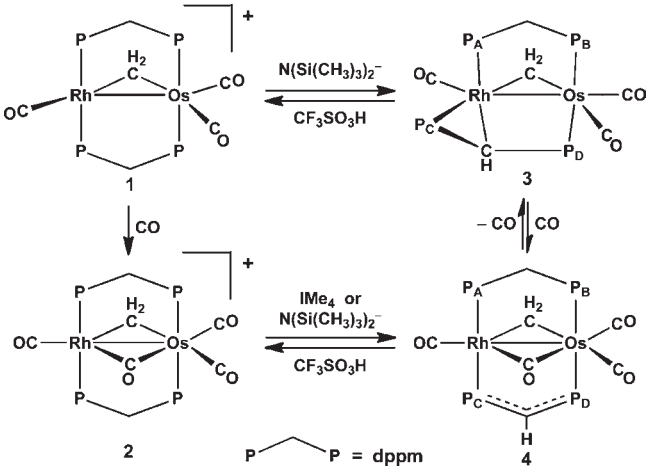


attached to Os opposite to the carbonyl ligand C1O1 and also refined with an occupancy factor of 50% and with a target Os−H1 distance of 1.60(1) Å. One solvent benzene molecule was situated with two mutual *p*-C atoms located on the crystallographic mirror plane (*x*, *y*, 0). Two other benzene molecules were found to be disordered across the mirror plane (*x*, *y*, $^1/_2$); the atoms in each of these six carbon sets were refined with an occupancy factor of 50%. (iv) Yellow crystals of **7a** were obtained by the slow diffusion of hexanes into a $CH_2Cl_2$ solution containing the product. Compound **7a** exhibits two independent forms of disorder, one involving the interchange of the Rh and Os positions and the other involving the position of the linked ketenyl/dppm-H groups, as shown in Figure 2. Both metal sites were refined as a mixture of Os and Rh, with the Os(A)/Rh(B) site modeled as $Os_{0.55}Rh_{0.45}$ and the Rh(A)/Os(B) site as $Rh_{0.55}Os_{0.45}$. As a result of the mixed occupancy of the metal sites, the C atom of the semibridging carbonyl ligand was split over two sites, with occupancies of 0.55 for C2A and 0.45 for C2B; the O atom was not disordered. The hydride ligand attached to the Os center was also necessarily disordered with the same occupancies as those described above. Finally, the carbonyl group linking the dppm-H and methylidyne C atoms was modeled as 60% bound between atoms C5 and C6 and 40% between atoms C5 and C7. The hydride ligands H1A and H1B were located from the difference Fourier map and their positions allowed to refine; the thermal parameters for the hydride atoms were constrained to be equal.

## RESULTS AND COMPOUND CHARACTERIZATION

**a. dppm Deprotonation.** As noted in the Introduction and diagrammed in Scheme 1, the reaction of the methylene-bridged species $[RhOs(CO)_3(\mu\text{-}CH_2)(dppm)_2][CF_3SO_3]$ with $IMe_4$ yields two products; the first, $[RhOs(IMe_4)(CO)_2(\mu\text{-}CH_2)(dppm)_2][CF_3SO_3]$,[1a] results from carbonyl substitution by $IMe_4$ and the other, compound **3**, results from dppm deprotonation by $IMe_4$. The deprotonation product **3** can be formed quantitatively from **1** by a reaction with the strong base $KN(Si(CH_3)_3)_2$, as shown in Scheme 2, avoiding the necessity of separating this product from the methylene-bridged, $IMe_4$-containing product.[1a]

Compound **3** appears in the $^{31}P\{^1H\}$ NMR spectrum as four resonances, consistent with an ABCDX spin system in which all phosphorus nuclei are chemically inequivalent. The resonances at $\delta$ 48.5 and −3.2, corresponding to $P_A$ and $P_C$, respectively (see Scheme 2 for labeling), display 143 and 87 Hz coupling to Rh, establishing their coordination to this metal, while the resonances at $\delta$ 6.5 and −7.2 show no Rh coupling and correspond to the Os-bound ends of the dppm and dppm-H ligands, respectively. The strong coupling of 282 Hz between $P_B$ and $P_D$ indicates that this pair of $^{31}P$ nuclei are mutually trans at Os, while the weak 18 Hz coupling between $P_A$ and $P_C$ (at Rh) indicates a mutually cis arrangement for these nuclei. The 89 Hz intraligand coupling ($^2J_{P_A-P_B}$) across the dppm bridge is normal; however, the intraligand $^{31}P-^{31}P$ coupling across the $Ph_2P_CCHP_DPh_2$ bridge, at 21 Hz, is significantly less than that for the dppm group and much less than has previously been observed in dppm-H compounds (ca. 140 Hz) in which this ligand maintains a $\mu\text{-}\kappa^1\text{:}\kappa^1$ geometry, binding to each metal via P.[1,2a,b]

In the $^1H$ NMR spectrum, a $\mu\text{-}^{13}CH_2$-enriched sample confirms that signals at $\delta$ 5.18 and 4.45 are due to the chemically inequivalent protons of this metal-bridged methylene group, with normal one-bond couplings to the labeled C atom of 134.5 and 140.8 Hz, respectively. The resonances at $\delta$ 4.62 and 3.47 are assigned to the inequivalent methylene protons of the intact


dx.doi.org/10.1021/ic102470j |*Inorg. Chem.* 2011, 50, 3523–3538

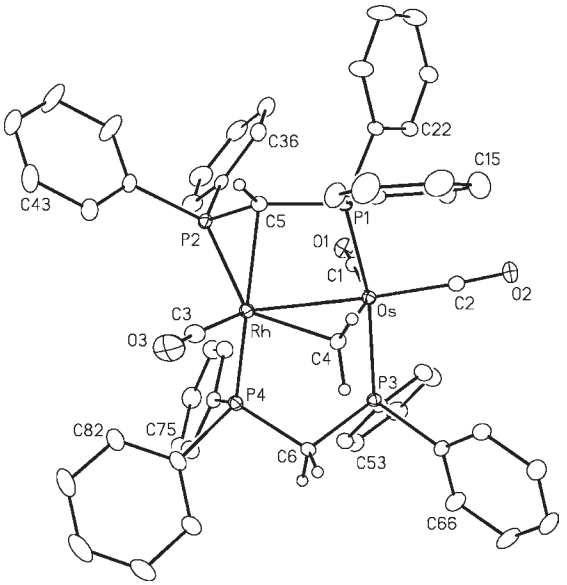


**Figure 3.** Perspective view of **3** showing the atom labeling scheme. Phenyl C atoms are numbered sequentially around the ring, starting from the *ipso*-C such that the first digit represents the ring number. Non-H atoms are represented by Gaussian ellipsoids at the 20% probability level. H atoms are shown with arbitrarily small thermal parameters for dppm methylene groups. Phenyl H atoms are omitted. Relevant parameters (distances in Å and angles in deg): Os−Rh = 2.7469(3), Os−P1 = 2.3385(8), Os−P3 = 2.3485(8), Os−C4 = 2.105(3), Rh−P2 = 2.3005(8), Rh−P4 = 2.2823(8), Rh−C4 = 2.147(3), Rh−C5 = 2.252(3), P2−C5 = 1.782(3), P1−C5 = 1.767(3); P2−Rh−C5 = 46.08(8)°, Rh−P2−C5 = 65.54(10)°, Rh−C5−P2 = 68.38(10)°, Rh−C5−P1 = 96.15(13)°, C5−P1−Os = 105.39(10)°.

dppm group, on the basis of $^{31}$P decoupling experiments, while the proton of the dppm-H methanide group appears upfield at $\delta$ 1.38 as a broad multiplet, in which selective $^{31}$P decoupling experiments confirm unresolved coupling to all four $^{31}$P nuclei. Broad-band $^{31}$P decoupling also sharpens the $^{1}$H signal for the $\mu$-$^{13}$CH$_2$ protons, allowing a weak 1.6 Hz coupling to Rh to be observed; two-bond Rh−H coupling of less than 3 Hz is typical.[8] Even with broad-band $^{31}$P decoupling, the dppm-H methanide resonance shows no resolved coupling to Rh.

In the $^{13}$C{$^{1}$H} NMR spectrum, both Os-bound carbonyl groups appear as pseudotriplets at $\delta$ 188.1 and 186.1, with approximately equal coupling to the adjacent inequivalent P nuclei, while the remaining carbonyl, at $\delta$ 188.2, appears as a doublet of multiplets with 65 Hz coupling to Rh. The bridging-methylene group, observed at $\delta$ 75.0 in the $^{13}$C{$^{1}$H} NMR spectrum, appears as a broad multiplet with coupling to the four chemically inequivalent P nuclei and to Rh (21 Hz). Although the dppm methylene signal is observed in the $^{13}$C{$^{1}$H} NMR spectrum at $\delta$ 40.0, the resonance belonging to the dppm-H methanide C atom was not observed.

The structure of compound **3** was established by an X-ray crystallographic study and a representation, is shown in Figure 3. The resulting (dppm-H) ligand functions as a $\mu$-$\kappa^1$:$\eta^2$ ligand, binding to Os through P1 and to Rh through C5 and P2, yielding highly strained four- and three-membered metallacycles. This uncommon binding mode for dppm-H has been observed previously.[15]

The four-membered Rh−Os−P1−C5 metallacycle, having the P1−C5 edge substantially shorter than the opposite Rh−Os edge [1.767(3) vs 2.7469(3) Å], shows the expected distortion from idealized angles in which the Os−Rh−C5 and Rh−Os−P1 angles [81.48(8)° and 72.02(2)°, respectively] deviate significantly from idealized 90° values, while the Rh−C5−P1 and Os−P1−C5 angles [96.2(1)° and 105.4(1)°, respectively] deviate from idealized tetrahedral values. Not surprisingly, the angles within the three-membered Rh−P2−C5 metallacycle [C5−Rh−P2 = 46.08(8)°; Rh−P2−C5 = 65.5(1)°; P2−C5−Rh = 68.4(1)°] deviate even more noticeably from the idealized, unconstrained values. The P−C(H) distances within the deprotonated and metalated (dppm-H) fragments [1.782(3) and 1.767(3) Å] are significantly shorter than the P−CH$_2$ distances within the intact dppm group [1.837(3) and 1.839(3) Å] but are still longer than those observed in dppm-H fragments that have not undergone metalation at the methanide C atom, for which distances ranging from 1.72(2) to 1.738(8) Å have been reported.[16] The Rh−C5 distance [2.252(3) Å] is long, probably because of the strain within this bridging ligand, and can be compared to the normal Rh−C4 and Os−C4 distances [2.147(3) and 2.105(3) Å] involving the bridging methylene group. Including the Rh−Os bond, the geometries at both metals can be described as highly distorted octahedra, with all major distortions resulting from the strain imposed by the three different metallacycles involved. The geometry involving this bridging (dppm-H) ligand in **3** compares closely to that reported for [Fe$_2$(CO)$_6$($\mu$-H)(dppm-H)].[15]

As shown in Scheme 2, under an atmosphere of CO, compound **3** readily converts into **4**, in which the added carbonyl has displaced the methanide C atom of the dppm-H ligand from Rh, to give the more conventional $\kappa^1$:$\kappa^1$ bridging mode for this deprotonated group (Scheme 2).[2,3] Compound **4** is unstable, reverting to **3** in the absence of CO and converting to other products (vide infra) under an atmosphere of CO at ambient temperature. For this reason, the NMR spectra of **4** were obtained at −80 °C. The $^{31}$P{$^{1}$H} NMR spectrum of **4**, like **3**, displays a four-resonance pattern for the four chemically inequivalent $^{31}$P nuclei. The Rh-bound $^{31}$P nuclei appear at $\delta$ 45.4 and 24.3 ($P_C$ and $P_A$; see Scheme 2 for labeling) and show coupling to Rh of 149 and 143 Hz, respectively, while the Os-bound $^{31}$P nuclei ($P_D$ and $P_B$) appear at $\delta$ 2.1 and −7.0. However, unlike the spectrum for **3**, that of **4** displays large $P_A$−$P_C$ and $P_B$−$P_D$ coupling of 253 and 226 Hz, respectively, establishing a mutually trans arrangement of dppm and dppm-H ligands at *both* metals. The large intraligand $P_C$−$P_D$ coupling within the dppm-H ligand of 125 Hz, compared to 89 Hz coupling within the dppm ligand, is also consistent with the delocalized P−C−P bonding shown, as discussed previously,[1,2a,2b] and establishes the change in dppm-H coordination upon the addition of CO.

In the $^{1}$H NMR spectrum of complex **4**, the presence of a pair of resonances at $\delta$ 4.08 and 3.32, corresponding to chemically inequivalent methylene protons of the dppm ligand, is consistent with the absence of front/back symmetry in the molecule, while the presence of two broad multiplets, at $\delta$ 2.24 and 2.20, assigned to the inequivalent protons of the bridging CH$_2$ group, is consistent with the additional absence of top/bottom symmetry in the complex. The methanide proton of the dppm-H group appears upfield at $\delta$ 0.44 as a broad multiplet, which sharpens upon broad-band $^{31}$P decoupling.

In the $^{13}$C{$^{31}$P,$^{1}$H} NMR spectrum of **4**, four carbonyl resonances are observed. The terminal, Rh-bound carbonyl, observed at $\delta$ 200.1, shows 24 Hz coupling to the $\mu$-$^{13}$CH$_2$


dx.doi.org/10.1021/ic102470j |*Inorg. Chem.* 2011, 50, 3523–3538

**Scheme 3**

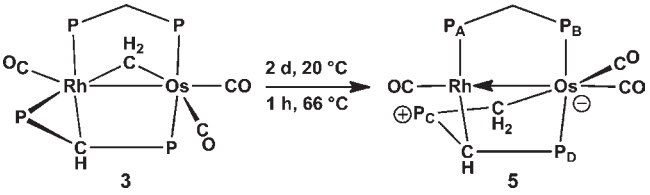


group, as confirmed from $^{13}C-^{13}C$ COSY correlations, suggesting a mutually trans arrangement of these groups, and also displays 59 Hz coupling to $^{103}Rh$. The $\mu$-CO group, observed at $\delta$ 215.0, shows trans C−C coupling of 16 Hz to an Os-bound carbonyl, the resonance for which appears at $\delta$ 182.1 (confirmed by $^{13}C-^{13}C$ COSY correlations), and 32 Hz coupling to $^{103}Rh$, suggesting a symmetrically bridged geometry. The remaining Os-bound carbonyl is observed at $\delta$ 181.4, while the bridging $\mu$-$CH_2$ group is located at $\delta$ 35.7 as a broad multiplet, for which Rh coupling was unresolved.

Whereas the reaction of the tricarbonyl species (**1**) with $IMe_4$ results in competing deprotonation and coordination to give the pair of products shown in Scheme 1, the reaction of the tetracarbonyl analogue (**2**) with $IMe_4$ results in the exclusive formation of **4**, in which $IMe_4$ has functioned solely as a Brønsted base (Scheme 2). Not surprisingly, compound **4** can also be synthesized cleanly from **2** using the strong base KN(Si-$(CH_3)_3)_2$. Protonation of either **3** or **4** with triflic acid regenerates the respective precursors **1** and **2**.

**b. Subsequent Transformation of Compound 3.** Compound **3** can be kept indefinitely at −30 °C but transforms slowly in solution at ambient temperature to the novel species **5** as diagrammed in Scheme 3, in which the Rh-bound end of the dppm-H group has migrated to the bridging-$CH_2$ ligand. This transformation occurs within 1 h in refluxing THF. In the $^{31}P\{^1H\}$ NMR spectrum of **5**, four resonances are again observed; the signals at $\delta$ 29.1 and −2.2 are assigned to $P_A$ and $P_B$, respectively, of the dppm bridge (see Scheme 3 for labeling), while the signals at $\delta$ 12.4 and 0.2 are assigned to $P_C$ and $P_D$, respectively, of the bridging $Ph_2PCHPPh_2CH_2$ ligand. The small coupling (6 Hz) of $P_C$ to Rh indicates that this P is no longer Rh-bound and can be contrasted with the $^1J_{RhP}$ value of 165 Hz involving $P_A$. The large mutual coupling of 255 Hz between the $P_B$ and $P_D$ nuclei and their lack of Rh coupling indicate their mutually trans arrangement on Os. The intraligand $^{31}P-^{31}P$ couplings for $P_A-P_B$ and $P_C-P_D$, through the dppm methylene and coordinated methanide bridge, are comparable at 77 and 70 Hz, respectively.

In the $^1H$ NMR spectrum, the chemically inequivalent protons of the dppm methylene group appear as multiplets at $\delta$ 5.29 and 4.57, which collapse to a pair of doublets upon broad-band $^{31}P$ decoupling, revealing mutual coupling of 15.2 Hz, while the coordinated methanide proton, appearing at $\delta$ 4.19 as a broad multiplet, sharpens to a doublet with broad-band $^{31}P$ decoupling, revealing 1.9 Hz coupling to Rh. The $^1H$ resonances at $\delta$ 1.84 and 1.64 are assigned to the unique Os-bound $CH_2$ protons and appear as sharp multiplets, which upon broad-band $^{31}P$ decoupling collapse to an AB quartet displaying mutual coupling of 13.6 Hz. In a series of selective $^{31}P$ decoupling experiments, it was shown that these two protons are coupled to the three adjacent $^{31}P$ nuclei ($P_B$, $P_C$, and $P_D$) but not to the remote P ($P_A$) or to Rh.

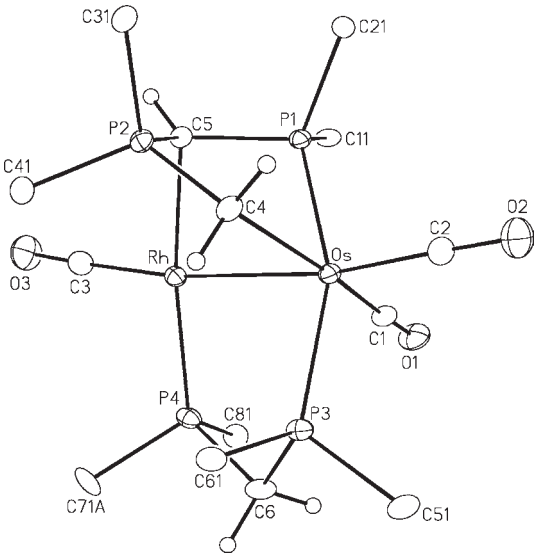


**Figure 4.** Perspective view of **5** showing the atom labeling scheme. Atom numbering and thermal parameters are as described for Figure 3. For the phenyl groups, only the *ipso*-C atoms are shown. Relevant parameters (distances in Å and angles in deg): Os−Rh = 2.7679(4), Os−P1 = 2.3214(8), Os−C4 = 2.241(4), Rh−C5 = 2.170(3), P2−C4 = 1.786(3), P2−C5 = 1.752(3), P1−C5 = 1.782(3); P1−Os−Rh = 67.38(2)°, C5−Rh−Os = 78.61(8)°, C5−P1−Os = 99.97(11)°, C5−P2−C4 = 107.62(16)°, Rh−C5−P1 = 91.65(13)°, Rh−C5−P2 = 97.31(14)°, P2−C5−P1 = 107.47(17)°, P2−C4−Os = 110.90(16)°.

In the $^{13}C\{^1H\}$ spectrum of a $^{13}CO$- and $^{13}CH_2$-enriched sample of **5**, the Os-bound carbonyl at $\delta$ 190.0 shows trans coupling to the methylene C atom of 13 Hz and coupling to both Os-bound phosphines ($P_B$ and $P_D$) of 9 Hz. The narrow multiplet at $\delta$ 186.2 for the other Os-bound carbonyl shows no coupling to either the other Os-bound carbonyl or the $^{13}CH_2$ group, while the remaining signal at $\delta$ 188.7 is assigned to the Rh-bound carbonyl on the basis of distinctive one-bond coupling of 72 Hz to this metal and its cis coupling to $P_A$ of 11 Hz. The $^{13}CH_2$ group, observed at $\delta$ −22.6, appears as a multiplet, showing one-bond coupling to $P_C$ (45 Hz) and 5 Hz cis coupling to the adjacent Os-bound phosphines, $P_B$ and $P_D$. The proton-coupled $^{13}C$ NMR spectrum reveals equal 132 Hz coupling to the chemically distinct protons, consistent with observations in the corresponding $^1H$ NMR spectrum.

The structure shown for **5** in Scheme 3 was established by an X-ray structure determination, and a representation of the complex is shown in Figure 4. A comparison of the structures of **3** and **5** suggests that the observed transformation is favored by the conversion of two highly strained three-membered metallacycles (involving the methylene bridge and the C-metalated dppm-H group) in **3** into a much less strained five-membered ring involving the coupled dppm-H and $CH_2$ groups in **5** in which all angles at C and P approach the favored tetrahedral values. The significance of the shorter P2−C5 distance [1.752(3) Å] compared to P1−C5 and P2−C4 [1.782(3) and 1.786(3) Å, respectively] is not clear. The major change in the dppm-H fragment upon transformation of **3** to **5** is the closing of the P1−C5−P2 angle from 127.1(2)° to 107.5(2)°, presumably a reflection of the relief of strain upon decomplexation of P2 from Rh. Within the remaining four-membered Os−P1−C5−Rh dimetallacycle, the parameters have changed little from the values in **3**. P2 is clearly beyond the bonding distance to Rh,


dx.doi.org/10.1021/ic102470j |*Inorg. Chem.* 2011, 50, 3523–3538

**Scheme 4**

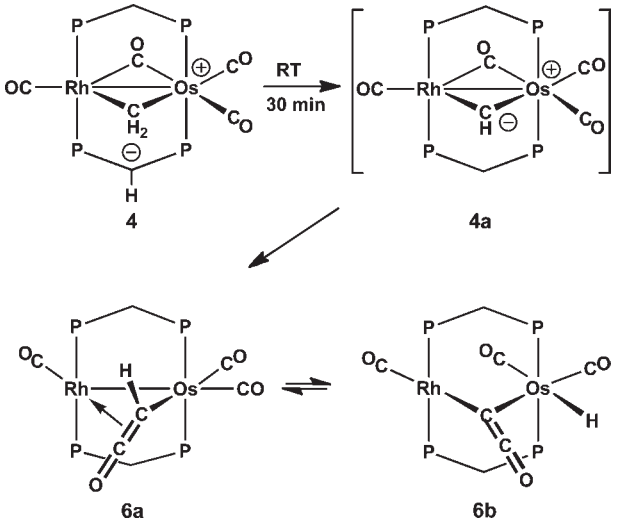


being 2.9576(9) Å from this metal. Interestingly, the Rh−C5 distance in **5** [2.170(3) Å] is significantly shorter than that in the precursor **3** [2.252(3) Å], presumably reflecting the relief of strain, alluded to earlier, in the transformation to **5**, whereas the Os−C4 distance [2.241(4) Å] has lengthened substantially from that in **3** [2.105(3) Å].

Although we have not seen structures involving phosphonium ylide complexes of Os, those reported for complexes of Rh,[17a] Pd,[17b,c] and Pt[17d] display significantly shorter M−C distances in the range 2.031−2.185 Å. Presumably, the long Os−$CH_2$ distance in **5** reflects the weakness of this dative bond from the ylide C to the Os(0) center.

**c. Transformations Involving Compound 4.** As noted above, compound **3** converts to **4** in the presence of CO by CO displacement of the Rh-bound dppm-H/methanide C and is readily regenerated in the absence of CO. However, even under an atmosphere of CO, compound **4** is unstable, converting over a 30 min period to a mixture of two species, proposed to be the pair of ketenyl- and ketenylidene-bridged/hydride tautomers **6a** and **6b**, respectively, in nearly equal portions, as outlined in Scheme 4. Apparently, proton transfer between the bridging methylene group of **4** and the methanide C of dppm-H occurs, generating a bridging methylidyne group. The putative, methylidyne-bridged intermediate (**4a**) is never observed, converting instead to the ketenyl-bridged species **6a** via coupling of the methylidyne group with a carbonyl ligand, as outlined in Scheme 4. The tautomer **6b** is presumably generated from **6a**, by a facile, reversible transfer of the α-H.

In attempts to determine whether proton transfer between the $\mu$-$CH_2$ group and dppm-H in **4**, to give **4a**, was reversible, spin-saturation-transfer experiments were carried out. However, irradiation of the $\mu$-$CH_2$ proton resonances at ambient temperature resulted in no change in the intensity of any other resonances. Furthermore, a sample of $[RhOs(CO)_4(\mu\text{-}CD_2)(\mu\text{-}\kappa^1{:}\kappa^1\text{-dppm-H})(dppm)]$ (**4-$CD_2$**) showed no deuterium incorporation into the dppm methylene groups until **6a** and **6b** began appearing. It appears that proton transfer is slow compared to subsequent coupling of the methylidyne fragment and a carbonyl.

In the $^{31}P\{^1H\}$ NMR spectrum of **6a** at ambient temperature, only two resonances appear, with the Rh-bound ends of the dppm groups appearing at $\delta$ 13.8 ($^1J_{PRh}$ = 142 Hz) and the Os-bound ends at $\delta$ −0.2. Cooling below ambient temperature results in a broadening of the signals for the Rh-bound $^{31}P$ nuclei, and by −40 °C, this signal has collapsed into the baseline, while the signal for the Os-bound ends appears unaltered. At −60 °C, the Os-bound $^{31}P$ signal also begins to broaden, and at −80 °C, four broad resonances of equal intensity appear at $\delta$ 21.0, 9.3, 2.0, and 0.9, with the first two corresponding to the Rh-bound ends of the diphosphines. This four-resonance pattern is as expected for **6a** on the basis that the orientation of the ketenyl group, as shown in Scheme 4, would give rise to "top/bottom" asymmetry while the "left/right" asymmetry results from the differences in the metals. The fluxionality observed presumably involves rotation about the Os−C bond, moving the ketenyl group from the "bottom" position shown to the "top" position, and clearly has a greater influence on the Rh-bound $^{31}P$ nuclei, as seen from the greater separation in the chemical shifts.

Because of the lack of "front/back" symmetry about the $RhOsP_4$ plane in **6a**, the dppm methylene protons appear as multiplets at $\delta$ 4.57 and 4.08 in the $^1H$ NMR spectrum, and broad-band $^{31}P$ decoupling simplifies these multiplets to doublets with mutual coupling of 14.5 Hz. On the basis of the geometry shown for **6a**, four separate resonances are to be expected for these methylene protons at low temperature. However, even at −80 °C, the two-signal pattern persists, although at this temperature, these signals are broad. The failure to resolve the expected four resonances is possibly not surprising given that the $^{31}P$ resonances were not resolved until near −80 °C, and these nuclei should be more influenced by the ketenyl orientation because of their proximity to this group. In a $^{13}CO$- and $^{13}CH$-enriched sample of **6a**, the ketenyl proton appears as a doublet of triplets of triplets of doublets at $\delta$ 4.28, in which the one-bond C−H coupling of 169 Hz agrees with the proposed connectivity shown. Selective $^{31}P$ decoupling reveals 8.4 Hz coupling of this proton to the Os-bound ends of the diphosphines and 4.9 Hz coupling to the Rh-bound ends; broad-band $^{31}P$ decoupling also allows the observation of 3.6 Hz coupling to $^{103}Rh$.

Four carbonyl resonances are observed in the $^{13}C\{^1H\}$ NMR spectrum, corresponding to the three carbonyl ligands and the ketenyl carbonyl group. The resonance at $\delta$ 191.3 appears as a doublet of triplets displaying 69 Hz coupling to $^{103}Rh$ and 14 Hz coupling to the Rh-bound $^{31}P$ nuclei, establishing this as a terminally bound carbonyl on Rh. The two other carbonyl ligands are Os-bound, displaying no Rh coupling; the signal at $\delta$ 193.1 displays no obvious coupling to the $^{31}P$ nuclei and appears as a doublet in the $^{13}CH$-labeled sample with 13 Hz coupling to the α-C of the ketenyl group, consistent with a mutually trans arrangement of these ligands, while the signal at $\delta$ 182.5 is a triplet displaying 8 Hz coupling to the Os-bound $^{31}P$ nuclei. For the bridging ketenyl group, the carbonyl resonance appears at $\delta$ 214.6 while the methyne C appears at $\delta$ 22.0. Broad-band $^{31}P$ decoupling shows mutual one-bond $^{13}C-^{13}C$ coupling of 52 Hz between these two ketenyl C atoms, confirming their connectivity, and additional Rh coupling to these C atoms (9 and 7 Hz, respectively) supports the proposed $\eta^2$-coordination mode to this metal. These $^{13}C$ resonances can be compared to the values reported for $[Fe_2(CO)_8(\mu\text{-Cl})(\mu\text{-CHCO})]$ [$\delta$: $C_\alpha$ = −4 (d), $C_\beta$ = 162 (s)][18] and $[(Cp(CO)Fe)_2(\mu\text{-CHCO})]^+$ [$\delta$: $C_\alpha$ = 27.5 ($^1J_{CH}$ = 174 Hz), $C_\beta$ = 162.6 (s)].[19]

The other tautomer present in solution, **6b**, appears as two resonances in the $^{31}P\{^1H\}$ NMR spectrum, remaining virtually unchanged over the temperature range from ambient to −80 °C.


dx.doi.org/10.1021/ic102470j |*Inorg. Chem.* 2011, 50, 3523–3538

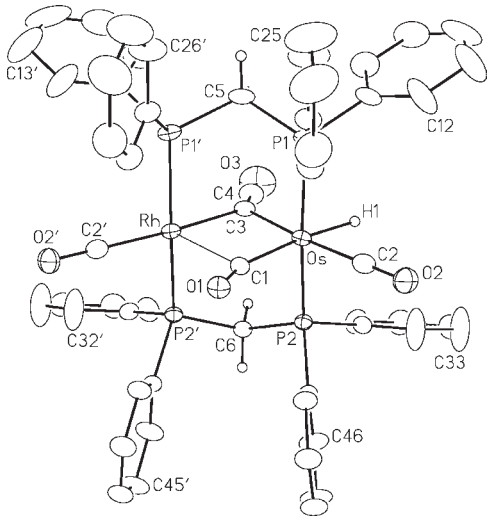


**Figure 5.** Perspective view of one of the disordered molecules of **6b** showing the atom labeling scheme. Phenyl C atoms are numbered sequentially around the ring, starting from the *ipso*-C such that the first digit represents the ring number. Non-H atoms are represented by Gaussian ellipsoids at the 20% probability level. H atoms are shown with arbitrarily small thermal parameters for the hydrido ligand (H1) and dppm methylene groups. Phenyl H atoms are omitted for clarity. Primed atoms are related to unprimed ones via the crystallographic mirror plane ($x$, $y$, 0), upon which the O1, O3, C3, C4, C5, and C6 atoms are located. Relevant parameters (distances in Å and angles in deg): Rh−Os = 2.9948(4), Rh−C1 = 2.419(6), Os−C1 = 2.003(6), Os−C2 = 1.858(4), Os−C3 = Rh−C3 = 2.120(3), Os−H1 = 1.595(10), C3−C4 = 1.232(7), C4−O3 = 1.206(7); C1−Os−C2 = 90.0(2)°, C1−Os−C3 = 98.61(19)°, C2−Os−C3 = 171.26(14)°, C1−Os−H1 = 172(2)°, C2−Os−H1 = 82(2)°, C3−Os−H1 = 89(2)°, Os−C1−Rh = 84.7(2)°, Os−C1−O1 = 158.9(5)°, Rh−C1−O1 = 116.4(4)°, Os−C2−O2 = 177.9(3)°, Os−C3−Rh = 89.86(17)°, Os−C3−C4 = 134.67(10)°, Rh−C3−C4 = 134.67(10)°, C3−C4−O3 = 178.5(7)°.

At ambient temperature, the Rh-bound $^{31}$P nuclei appear as a multiplet at $\delta$ 26.3 displaying 144 Hz coupling to $^{103}$Rh, while the Os-bound ends of the diphosphines appear at $\delta$ −3.6. In the $^{1}$H NMR spectrum for **6b**, the hydride signal appears as a triplet of triplets at $\delta$ −7.01, and selective $^{31}$P decoupling establishes 20.9 Hz coupling to the Os-bound $^{31}$P nuclei and only 2.5 Hz to the Rh-bound $^{31}$P nuclei. Together with the absence of Rh coupling, this suggests that this hydride is terminally bound to Os. The dppm methylene protons appear as expected.

In a sample prepared from $^{13}$CO- and $^{13}$CH$_2$-enriched **4**, four carbonyl resonances are observed for tautomer **6b** in the $^{13}$C-{$^{1}$H} NMR spectrum, corresponding to the three carbonyl ligands and the ketenylidene carbonyl group. The Rh-bound carbonyl, at $\delta$ 195.4 ($^{1}J_{CRh}$ = 69 Hz), and an Os-bound carbonyl, at $\delta$ 182.2, each show two-bond coupling to the ketenylidene α-C of 22 and 15 Hz, respectively, suggesting a trans arrangement of these carbonyls with respect to the ketenylidene group at the respective metals. The third carbonyl ligand, at $\delta$ 186.6, is also Os-bound; the absence of coupling of this carbonyl to the ketenylidene α-C and large trans coupling to the terminal Os-bound hydride (17 Hz), in the proton-coupled spectrum, indicate that this carbonyl occupies the site on Os opposite the hydride. No obvious $^{103}$Rh coupling is observed in this carbonyl signal, although the X-ray structure indicates a semibridging interaction with this metal in the solid state (vide infra). The ketenylidene carbonyl group, appearing as a sharp doublet at $\delta$ 160.6 in a $^{13}$C═$^{13}$C═O sample, and the dimetalated carbon, at $\delta$ −5.5, show mutual 112 Hz $^{13}$C−$^{13}$C coupling, confirming their connectivity. The signal for the α-C of the ketenylidene group appears as a complex multiplet because of the additional $^{13}$C coupling resulting from $^{13}$CO labeling. Broad-band $^{31}$P decoupling simplifies this multiplet, allowing 22 Hz coupling to $^{103}$Rh to be discerned. The chemical shifts of these ketenylidene C atoms and their mutual coupling agree with literature findings for such moieties. For example, the reported $^{13}$C resonances for [($\mu$-H)$_2$Os$_3$(CO)$_9$($\mu_3$-CCO)] are at $\delta$ 8.6 and 160.3, with mutual $^{13}$C−$^{13}$C coupling of 86 Hz,[20] while for [($\mu$-H)$_2$Ru$_3$(CO)$_9$($\mu_3$-CCO)], the corresponding resonances are observed at $\delta$ 38.7 and 158.8, with mutual $^{13}$C−$^{13}$C coupling of 78 Hz.[21,22]

The IR spectrum for the ketenylidene-bridged species (**6b**) was obtained from crystalline samples and displays four bands at 2011, 1953, 1932, and 1904 cm$^{-1}$. We were unable to unambiguously assign one of these bands to the ketenylidene carbonyl, but note that any one of these are comparable to observed stretches in known ketenylidene-containing species,[23] being lower than the stretching frequency reported for free ketene (2133 cm$^{-1}$).[24] Dissolution of these crystals in THF-$d^8$ reestablishes the tautomeric equilibrium described above, as determined from multinuclear NMR spectroscopy. In addition to the bands established for **6b**, the solution IR spectrum now displays an additional broad absorption at 1964 cm$^{-1}$ and a strong adsorption at 1775 cm$^{-1}$. The former is assigned to a terminal carbonyl on **6a**, while the latter is likely due to the ketenyl carbonyl. Casey et al. reported the carbonyl absorption for the symmetrically bridged ketenyl group in [(Cp(CO)Fe)$_2$($\mu$-CHCO)]$^+$ at 2092 cm$^{-1}$.[19a,b] The significantly lower ketenyl stretch in **6a** is consistent with the proposed $\kappa^1$:$\eta^2$-coordination mode for this group. Furthermore, the ketenyl species reported by Casey et al. is fundamentally different from that of **6a**, being formed by CO attack at a cationic, electrophilic methylidyne group.

The X-ray structure determination of **6b** was carried out, and a view of this species, shown in Figure 5, confirms the structure proposed on the basis of the spectroscopic data and shows the bridging ketenylidene ligand lying in the equatorial plane with the carbonyl groups and the hydride ligand. Although this structure is disordered across the crystallographic mirror plane passing through the dppm methylene groups and the ketenylidene group, only the metals, the semibridging carbonyl, and the hydride are affected, so this disorder was readily resolved as described in the Experimental Section.

As shown in Figure 5, Rh has a square-planar geometry, while that of Os is octahedral; the long Rh−Os separation of 2.9948(4) Å is consistent with the absence of a metal−metal bond. The significant asymmetry in the bonding of the semibridging carbonyl, in which the Rh−C1 separation [2.419(6) Å] is much larger than the Os−C1 distance of 2.003(6) Å, is consistent with a weak interaction of this (primarily Os-bound) group with Rh. However, the slightly bent arrangement of the Os−C1−O1 unit [158.9(5)°] suggests a semibridging interaction, which causes a deviation from the linear arrangement expected for a terminal carbonyl. The lack of resolved $^{103}$Rh coupling to this carbonyl in the $^{13}$C{$^{1}$H} NMR spectrum suggests that this interaction remains weak in solution. The significant lengthening of the Os−C1 distance over the Os−C2 distance [2.003(6) vs. 1.858(4) Å] is probably due to the high trans influence of the hydride ligand. As required by the disorder, the Rh−C3 and Os−C3 distances [2.120(3) Å] of the $\mu$-ketenylidene group are identical, disguising any expected asymmetry resulting from the


dx.doi.org/10.1021/ic102470j |*Inorg. Chem.* 2011, 50, 3523–3538

**Table 2. C−C and C−O Distances in Ketene-Related Species**

| compound | C−C (Å) | C−O (Å) | ref |
|---|---|---|---|
| $[RhOs(H)(CO)_3(\mu\text{-}CCO)(dppm)_2]$ (**6b**) | 1.232(7) | 1.206(7) | this work |
| $[Cp(CO)Fe(\mu\text{-}CHCO)Fe(CO)Cp][PF_6]$ | 1.338(8) | 1.135(7) | 19a, 19b |
| $[(\mu\text{-}H)_2Os_3(CO)_9(\mu\text{-}CCO)]$ | 1.264(37) | 1.154(34) | 20 |
| $[Ph_4As]_2[Fe_3(CO)_9(\mu\text{-}CCO)]$ | 1.28(3) | 1.18(3) | 25 |
| $CH_2{=}C{=}O$ | 1.31(1) | 1.16(1) | 26 |

different metals and their different geometries, but, nevertheless, appear normal. The CCO moiety is close to linear [C3−C4−O3 = 178.5(7)°] with C3−C4 = 1.232(7) Å and C4−O3 = 1.206(7) Å. However, it should be noted that the nature of the disorder could disguise a slightly more bent arrangement that may be masked by the somewhat larger thermal ellipsoid for O3. Nevertheless, the parameters are in reasonable agreement with those of other ketene-related moieties, included in Table 2.

A $^1$H NMR spin-saturation-transfer experiment in which the hydride resonance of **6b** was irradiated resulted in no observable change in the appearance of the signal assigned to the CH group of **6a**. Assuming that a [1,2]-hydride migration is occurring, the failure to observe saturation transfer suggests that $T_1$ relaxation is occurring much more quickly than hydrogen transfer.

Solutions containing a mixture of compounds **6a** and **6b** under a CO atmosphere can yield the known complex $[RhOs(CO)_4(dppm)_2]^+$, as the acetate salt, as a minor impurity owing to hydrolysis of the ketenyl and/or ketenylidene fragments by adventitious water. The deliberate addition of water to this mixture of isomers generates this product rapidly and quantitatively at ambient temperature. The $[RhOs(CO)_4(dppm)_2]^+$ cation shows $^{13}$C, $^1$H, and $^{31}$P{$^1$H} chemical shifts in the NMR spectra nearly identical with what has already been reported for the $BF_4^-$ salt of this species.[9]

The equilibrium mixture of **6a** and **6b** in a carefully dried solution transforms under ambient conditions over a 7 day period to **7a** in nearly quantitative yield, as outlined in Scheme 5. This unusual transformation can be accelerated by heating the solution containing both isomers in benzene to 80 °C, resulting in full conversion within 30 min. However, under these conditions, **7a** is not obtained pure because conversion to **7b** (vide infra) is also occurring.

In the $^{31}$P{$^1$H} NMR spectrum of **7a**, four separate resonances are observed, indicating that all $^{31}$P nuclei are chemically inequivalent. The Rh-bound $^{31}$P nuclei, at $\delta$ 35.2 and −9.2, are identified by their coupling to $^{103}$Rh (154 and 138 Hz, respectively), while the Os-bound resonances appear at $\delta$ 4.8 and −28.9. The $^{31}$P NMR resonances in the substituted-dppm group show a significant upfield shift with respect to the unaltered dppm group, and the mutual coupling of the pair of Rh-bound (303 Hz) and Os-bound $^{31}$P nuclei (249 Hz) suggests a trans arrangement of the diphosphine groups at each metal. Whereas the intact dppm group shows a typical intraligand $^{31}$P−$^{31}$P coupling of 80 Hz, the analogous coupling within the modified diphosphine is surprisingly small (26 Hz). A similarly small $^2J_{PP}$ within the dppm-H ligand was noted earlier upon metalation of the methanide C in **3**.

In the $^1$H NMR spectrum of **7a**, five distinct proton resonances appear (in addition to the phenyl protons). The dppm methylene protons, at $\delta$ 3.24 and 2.74, simplify to an AB quartet upon broad-band $^{31}$P decoupling, distinguishing mutual 14.1 Hz coupling from 11 and 10 Hz coupling, respectively, to the adjacent $^{31}$P nuclei. The hydride, appearing as a complex

**Scheme 5**

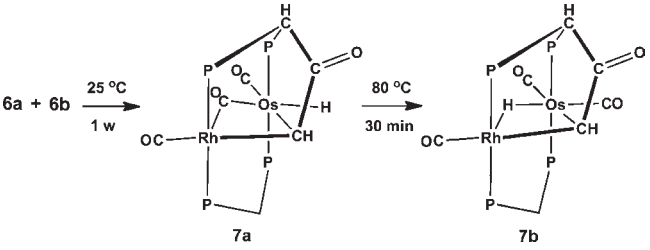


multiplet at $\delta$ −7.58, couples to the Os-bound (20 Hz) and Rh-bound (5 Hz) $^{31}$P nuclei, as determined by selective $^{31}$P decoupling experiments and shows an additional 1.5 Hz three-bond coupling to the $^1$H nucleus of the $\mu$-$^{13}$CH group (confirmed by $^1$H−$^1$H COSY correlations), 4 Hz coupling to $^{103}$Rh, and 15 Hz coupling to an Os-bound carbonyl (in the $^{13}$CO-enriched sample), supporting a mutually trans arrangement of the hydride and this CO. The $\mu$-$^{13}$CH group, at $\delta$ 4.10 in the $^1$H NMR spectrum, shows one-bond coupling to the $^{13}$C nuclei of 142 Hz consistent with an sp$^3$-hybridized carbon, while the $^1$H resonance at $\delta$ 4.16, assigned to the modified dppm-H bridging group, shows weak $^2J$ coupling to the pair of adjacent $^{31}$P nuclei of approximately 8 Hz and three-bond 8 Hz coupling to the $^{13}$C nuclei of the $\mu$-$^{13}$CH group (determined by broad-band $^{31}$P decoupling and selective $^{13}$C decoupling). This coupling would presumably be absent if not for the carbonyl linker connecting these bridging groups.

In the proton-coupled $^{13}$C NMR spectrum of **7a**, three carbonyl ligand resonances are observed. The terminal Rh-bound carbonyl, at $\delta$ 200.3, shows coupling to $^{103}$Rh of 63 Hz, to the Rh-bound $^{31}$P nuclei of 16 Hz, and to the $^{13}$C nuclei of the $\mu$-$^{13}$CH group of 17 Hz, supporting the mutually trans arrangement of the CO and $\mu$-CH groups. The semibridging carbonyl, at $\delta$ 197.2, displaying weak 3 Hz coupling to $^{103}$Rh, shows further coupling of 15 Hz to the Os-bound hydride and unresolved coupling of less than 2 Hz to Os-bound $^{31}$P nuclei, as determined from selective $^{31}$P decoupling. The remaining carbonyl group, at $\delta$ 183.8, is terminally bound to Os, showing coupling to the Os-bound $^{31}$P nuclei of 8 Hz, to the $^{13}$C nuclei of the $\mu$-$^{13}$CH bridging group of 11 Hz, and to the $^1$H nuclei of the substituted dppm-H bridge of 8 Hz. The ketonic carbonyl group, at $\delta$ 210.9, linking both bridging $^{13}$CH and dppm-H groups, shows one-bond coupling of 49 Hz to the $^{13}$C nucleus of the $\mu$-$^{13}$CH group, supporting the direct attachment of these groups. This ketonic group also shows equivalent coupling to the Rh- and Os-bound ends of the attached diphosphine of 16 Hz. In the proton-coupled $^{13}$C{$^{31}$P} broad-band spectrum, the resonance at $\delta$ 66.8, assigned to the metal-bridged $^{13}$CH group, confirms the 49 Hz coupling to the ketonic connecting group and 145 Hz C−H coupling, as well as the 16 and 11 Hz coupling to the Rh- and Os-bound carbonyls, respectively, that lie opposite this group, as noted above. This C also displays 16 Hz coupling to Rh.

The IR spectrum of **7a** is in agreement with the above NMR spectra, displaying stretches for two terminal and one bridging CO at 2017, 1957, and 1798 cm$^{-1}$; a band at 1587 cm$^{-1}$ is assigned to the bridging ketonic moiety.

As noted earlier and as shown in Figure 2, the structure of **7a** is disordered. The major contributing structure (A) is shown in Figure 6, confirming the structure proposed on the basis of spectroscopy. The very slight differences between the two


dx.doi.org/10.1021/ic102470j |*Inorg. Chem.* 2011, 50, 3523–3538

**Table 3. Selected Bond Lengths and Angles for Compound 7a**

| molecule A[a] | | | | molecule B[a] | | | |
|---|---|---|---|---|---|---|---|
| Distance (Å) | | | | | | | |
| OsA−RhA | 2.9735(3) | RhA−C2A | 2.417(9) | OsB−RhB | 2.9735(3) | RhB−C2B | 2.361(11) |
| OsA−C1 | 1.852(4) | RhA−C5 | 2.177(4) | OsB−C3 | 1.844(4) | RhB−C5 | 2.199(4) |
| OsA−C2A | 1.998(10) | C4A−C5 | 1.546(7) | OsB−C2B | 1.982(11) | C4B−C5 | 1.620(10) |
| OsA−C5 | 2.199(4) | C4A−C6 | 1.698(7) | OsB−C5 | 2.177(4) | C4B−C7 | 1.788(11) |
| OsA−H1A | 1.59(7) | C4A−O4A | 1.209(7) | OsB−H1B | 1.67(9) | C4B−O4B | 1.224(11) |
| RhA−C3 | 1.844(4) | O2−C2A | 1.152(10) | RhB−C1 | 1.852(4) | O2−C2B | 1.194(12) |
| Angle (deg) | | | | | | | |
| C1−OsA−C2A | 89.5(3) | P2−C6−C4A | 96.5(3) | C3−OsB−C2B | 90.8(3) | P3−C7−C4B | 90.8(4) |
| C1−OsA−H1A | 89(3) | OsA−P1−C6 | 107.74(13) | C3−OsB−H1B | 89(3) | OsB−P4−C7 | 110.54(14) |
| C5−OsA−H1A | 81(3) | RhA−P2−C6 | 106.98(14) | C5−OsB−H1B | 81(3) | RhB−P3−C7 | 110.99(14) |
| C5−RhA−C3 | 169.43(16) | OsA−P3−C7 | 110.99(14) | C5−RhB−C1 | 169.56(15) | OsB−P2−C6 | 106.98(14) |
| OsA−C5−C4A | 112.5(3) | RhA−P4−C7 | 110.54(14) | OsB−C5−C4B | 105.9(4) | RhB−P1−C6 | 107.74(13) |
| RhA−C5−C4A | 109.2(3) | OsA−C2A−O2 | 158.9(7) | RhB−C5−C4B | 103.4(4) | OsB−C2B−O2 | 156.4(8) |
| P1−C6−P2 | 115.2(2) | RhA−C2A−O2 | 116.9(6) | P3−C7−P4 | 113.2(2) | RhB−C2B−O2 | 117.6(7) |
| OsA−C5−RhA | 85.60(13) | C5−C4A−O4A | 128.4(5) | OsB−C5−RhB | 85.60(13) | C5−C4B−O4B | 122.7(8) |
| P1−C6−C4A | 96.3(3) | C6−C4A−O4A | 118.3(5) | P4−C7−C4B | 92.0(3) | C7−C4B−O4B | 116.4(8) |
| | | C5−C4A−C6 | 113.3(4) | | | C5−C4B−C7 | 120.9(6) |

[a] See Figure 2 for labeling of the disordered molecules.

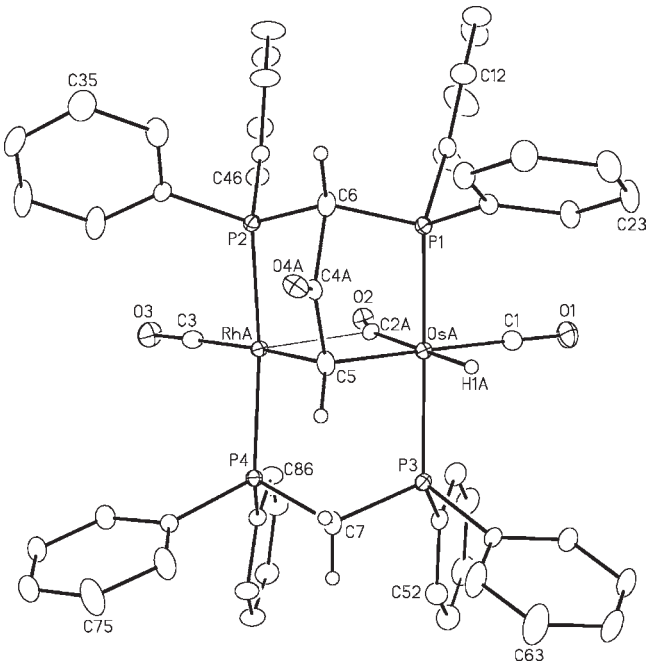


**Figure 6.** Perspective view of one of the disordered molecules of **7a** showing the atom labeling scheme. Atom numbering and thermal parameters are as described in Figure 3.

disordered molecules are attributed to packing, and only molecule A will be discussed further. The parameters for the other molecule (B) are given together with those of A in Table 3. For molecule A, the semibridging carbonyl is primarily bound to Os [OsA−C2A = 1.998(10) Å] while engaged in a weak semibridging interaction with Rh [RhA−C2A = 2.417(9) Å], causing a significant deviation from linearity in the OsA−C2A−O2 angle [158.9(7)°]. The hydride ligand was located and refined, yielding a typical Os−H distance of 1.59(7) Å.

The structure shown in Figure 6 is surprisingly close to those of conventional bis(dppm)-bridged complexes, except having the methanide C of the deprotonated dppm methylene group linked to the metal-bridged methylidyne group by an intervening carbonyl. The angles within this carbonyl-linked unit [OsA−C5−C4A = 112.5(3)°, RhA−C5−C4A = 109.2(3)°, C5−C4A−C6 = 113.3(4)°, P1−C6−C4A = 96.3(3)°, and P2−C6−C4A = 96.5(3)°] do not suggest a significant degree of strain. We assume that the unusually long distances involving this carbonyl group [C4A−C6 = 1.698(7) Å and C4A−C5 = 1.546(7) Å] are not chemically meaningful but are a consequence of the crystallographic disorder of this group. The ketenyl link involving the dppm-H group results in a slight bending of the P1−OsA−P3 and P2−RhA−P4 angles from linearity [162.06(3)° and 164.25(3)°, respectively] but, otherwise, shows no obvious distortions as a consequence of this linking fragment. This is not surprising considering the nature of the "top−bottom" disorder of this group, as discussed in the Experimental Section.

Refluxing **7a** in benzene results in isomerization to **7b** within approximately 30 min, as shown in Scheme 5. This isomerization has resulted from migration of the hydride ligand from its terminal position in **7a** to a bridging position in **7b**. The spectral parameters for **7b** are quite similar to those of **7a** (see Table 1) except that the new hydride resonance at $\delta$ −7.45 for **7b** now displays 17.1 Hz coupling to Rh and coincidental 9 Hz coupling to all four $^{31}$P nuclei, consistent with its bridging arrangement. Movement of the hydride from a terminal to a bridging position has been accompanied by the reverse transformation of the semibridging carbonyl, such that neither of the Os-bound carbonyls displays coupling to Rh. The ketonic linkage between the $\mu$-methyne C and the dppm-H methanide C displays spectral parameters similar to those of **7a**, indicating that this unit has remained intact.

The addition of 1 equiv of DMAD to a solution of **6a** and **6b**, in attempts to induce coupling of this alkyne to either the ketenyl or ketenylidene group, instead generates **8**, in which the added


dx.doi.org/10.1021/ic102470j |*Inorg. Chem.* 2011, 50, 3523–3538

**Scheme 6**

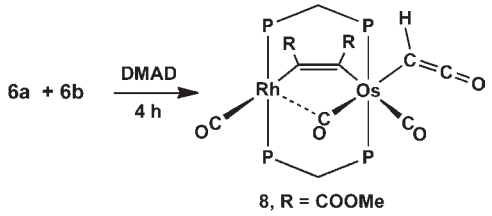


DMAD group bridges the metals, leaving the ketenyl group intact, but now in a terminal position, as shown in Scheme 6. In the $^{31}P\{^{1}H\}$ NMR spectrum, **8** appears as two multiplets with the Rh-bound ends of the diphosphines at $\delta$ 20.4 ($^{1}J_{PRh}$ = 157 Hz) and Os-bound ends at $\delta$ −6.8. In the $^{1}H$ NMR spectrum, the inequivalent $^{1}H$ nuclei of the dppm methylene groups, at $\delta$ 4.59 and 2.96, display mutual coupling of 14.5 Hz. A high-field resonance, at $\delta$ 0.59, assigned to the ketenyl CH group shows one-bond C−H coupling of 165.2 Hz in a $^{13}C$-enriched sample (prepared from $^{13}CH_2$-enriched **4**) and also shows additional coupling to the Os-bound phosphines of 3.6 Hz. Two singlets observed at $\delta$ 3.27 and 1.72 integrate as three protons each and are assigned to the methyl groups of the DMAD bridge.

In the $^{13}C\{^{1}H\}$ NMR spectrum, the terminal Rh-bound carbonyl group, at $\delta$ 194.2, displays 59 Hz coupling to this metal and 12 Hz coupling to the Rh-bound phosphines. One of the terminal CO groups bound to Os, at $\delta$ 195.2, shows 9 Hz coupling to $^{103}Rh$, 9 Hz two-bond coupling to the Os-bound phosphines, and a 21 Hz coupling to the $^{13}CH$-ketenyl group bound to Os, suggesting a mutually trans arrangement of these groups. The low-field shift of this carbonyl and its coupling to Rh suggests a semibridging arrangement. The other Os-bound CO, at $\delta$ 183.4, displays 7 Hz coupling to the Os-bound phosphines but no additional coupling. The ketenyl carbonyl group is observed as a sharp doublet of triplets at $\delta$ 180.8, with 96 Hz one-bond C−C coupling to the $^{13}CH$ group, confirming their connectivity, and 2 Hz three-bond coupling to the Os-bound phosphines. The absence of coupling to Rh and the increased coupling between the ketenyl C atoms, compared to **6a** (96 vs 52 Hz), is consistent with the proposed movement of this group from a bridging to a terminal site on Os. The high-field $^{13}C$ multiplet, at $\delta$ −19.1, is assigned to the CH group and appears in the proton-coupled spectrum as a doublet of doublets of doublets of triplets, owing to the C−H coupling (165 Hz), the coupling to the ketonic $^{13}CO$ (96 Hz), and the trans carbonyl (21 Hz) discussed above, and coupling to the Os-bound phosphines of 7 Hz. The resonances for the carboxylate groups of the DMAD moiety were resolved and appear as two singlets at $\delta$ 49.3 and 48.8 for the methyl groups and as a doublet of triplets at $\delta$ 177.6 ($^{2}J_{CRh} = {}^{3}J_{CP}$ = 2 Hz) and triplet at $\delta$ 165.3 ($^{3}J_{CP}$ = 2 Hz) for the carbonyl groups at the Rh and Os ends of the alkyne, respectively. The two resonances for the alkyne C atoms, at $\delta$ 183.7 and 155.2, each display coincidental ($^{2}J_{CP}$ or $^{3}J_{CP}$) coupling to all four $^{31}P$ nuclei of 11 and 6 Hz, respectively; in addition, the latter resonance displays coupling to Rh of 21 Hz, confirming its direct attachment to this metal.

In the IR spectrum, the low-frequency stretch at 1882 $cm^{-1}$ is assigned to the ketenic carbonyl, while the remaining bands (2026, 1971, and 1925 $cm^{-1}$) correspond to the carbonyl ligands. The carbonyl stretch for the coordinated DMAD appears at 1688 $cm^{-1}$. In the presence of water, compound **8** transforms to the known compound $[RhOs(CO)_3(\mu\text{-DMAD})(dppm)_2]^{+9}$ as the acetate salt, by hydrolysis of the ketenyl fragment.

## DISCUSSION

It is well recognized that NHCs, such as $IMe_4$, are basic, and a few reports outlining the deprotonation of acidic hydrocarbons by NHC groups have appeared.[4a,c,d] However, ligand deprotonation by an NHC is not common and, to our knowledge, has been reported on only a few occasions.[1,27] In two of these reports by our group, $IMe_4$ was observed to deprotonate acetonitrile, methyl, and dppm ligands in closely related Rh/Os systems.[1] In one of our reports,[1a] we proposed that restricted access of $IMe_4$ to the metals could inhibit its normal function as a ligand and instead favor its Brønsted basicity in which deprotonation could occur at a site remote from the crowded metal centers. The reactions of **1** and its carbonyl adduct **2** supports this proposal. In the case of the less crowded species **1**, both pathways, involving CO substitution by $IMe_4$ and dppm deprotonation by this group, are competitive, whereas in the more crowded tetracarbonyl species **2**, in which access of $IMe_4$ to the metals is less favorable, only the product of dppm deprotonation (**4**) is observed.

As noted earlier, deprotonation of the acidic dppm methylene protons is not unusual;[2,3] however, in most cases, the resulting methanide C either remains uncoordinated[2a,b,d−i,3] or coordinates to an exogenous metal that is not bound to the diphosphine ends of dppm-H.[28] We are aware of two previous examples having bonding of the dppm-H moiety related to that in **3**. In $[Fe_2H(CO)_6(\mu\text{-}\kappa^1\text{:}\eta^2\text{-dppm-H})]$,[15] a binding mode identical with that of **3** is observed, while for $[Pt_2(PPh_3)_2(\mu\text{-}\kappa^1\text{:}\kappa^1\text{-dppm-H})(\mu\text{-dppm})]^+$, the bridging dppm-H group binds to one metal via a $PPh_2$ moiety and to the other metal via the methanide C, in this case leaving the other $PPh_2$ end pendent and unattached to either metal.[2c]

Compound **3**, having the $\mu\text{-}\kappa^1\text{:}\eta^2$ binding mode of dppm-H, is highly strained and, as a consequence, is labile. In the presence of CO, displacement of the methanide C by CO occurs, converting the dppm-H group into its more commonly observed geometry in which it binds much like dppm, bridging through only the $PPh_2$ moieties. This transformation is reversible, and removal of CO regenerates compound **3**. Even in the absence of CO, compound **3** is unstable, presumably as a consequence of the internal strain, and rearranges to **5**, in which the Rh-bound $PPh_2$ moiety in the precursor has migrated to the bridging methylene group to give the diphosphino-ylide-bridged product shown in Scheme 2. It seems reasonable to assume that the conversion of **3** to **5** occurs by dissociation of the Rh-bound $PPh_2$ group from its highly strained three-membered ring to give a $\kappa^1\text{:}\kappa^1$ intermediate (similar to the structure of the diplatinum species noted above[2c]), followed by nucleophilic attack of this pendent phosphine at the bridging methylene group. However, such a transformation also requires inversion at the methanide C in order to bring the $PPh_2$ moiety to the same face of the "RhOs(diphosphine)" plane as the bridging methylene group (compare Figures 3 and 4). We propose that this "inversion" occurs via a planar "$RhOsP_4$" unit, as shown for species **3a** in Scheme 7. Such a transformation from a nonplanar to a planar "$RhOsP_4$" unit was observed in the conversion of **3** to **4**, under CO (Scheme 2). From this planar geometry, either recoordination of the methanide C can occur with the adjacent Rh-bound $PPh_2$ group returning to the original face to regenerate **3** or methanide group recoordination can


dx.doi.org/10.1021/ic102470j |*Inorg. Chem.* 2011, 50, 3523–3538

**Scheme 7**

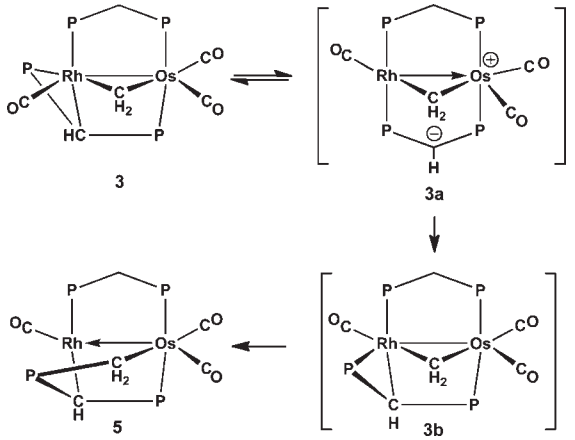


occur as shown in **3b**, placing the Rh-bound $PPh_2$ group adjacent to the bridging methylene group. In this position, $PPh_2$ dissociation followed by its attack at the adjacent bridging methylene group can occur to give **5**. Presumably, the conversion of **3** to **4** under CO (Scheme 2) also proceeds via intermediate **3a**, through CO coordination at the unsaturated Rh center, accompanied by migration of the other Rh-bound CO to a bridging site.

On the basis of the work by Sharp and co-workers, in which reversible proton transfer between an amido group and dppm-H was observed,[3a−d] we suggested that the bridging dppm-H group in **4** might be capable of deprotonating the accompanying bridging methylene group to give a reactive bridging methylidyne unit. This has been demonstrated in the subsequent reactivity of **4** under CO, although the putative $\mu$-CH-containing product was not observed. Instead, coupling of this methylidyne moiety with a CO ligand occurs to generate the ketenyl-bridged species (**6a**), which is in equilibrium with the ketenylidene-bridged, hydride tautomer (**6b**), as outlined in Scheme 3. The increased reactivity of a $\mu$-CH fragment over the $\mu$-$CH_2$ precursor was also observed by Casey et al.[19c] in which coupling of the methylidyne unit and a carbonyl was also observed. In the Casey study, the methylidyne-bridged intermediate was generated from the methylene-bridged precursor by hydride abstraction, and the ketenyl product resulted from nucleophilic attack at the electrophilic methylidyne unit by exogenous carbon monoxide, while in the present case, the ketenyl product results from nucleophilic attack of the methylidyne carbanion at a bound carbonyl ligand. The resulting $\mu$-$\kappa^1$:$\eta^2$ bridging mode for the ketenyl moiety, proposed for **6a**, was previously proposed by Pettit et al.[18] in $[Fe_2(CO)_6(\mu\text{-Cl})(\mu\text{-CHCO})]$, and such a bonding arrangement has more recently been confirmed in the phenyl-substituted ketenyl species $[MCo\{\mu\text{-C(CO)C}_6H_5\}(CO)_4(\eta\text{-C}_5H_5)]$ (M = Mn, Re).[29]

Although the ketenyl (**6a**) and ketenylidene/hydride (**6b**) tautomers are present in approximately equal proportions in solution, only **6b** is present in the solid state, and the X-ray structure determination of this product together with its NMR characterization unambiguously establishes the structure. When redissolved, the tautomeric equilibrium is quickly reestablished. Unfortunately, spin-saturation-transfer experiments failed to demonstrate exchange between the ketenyl proton and the Os-bound hydride ligand. The transformation of the ketenyl species (**6a**) to the ketenylidene tautomer (**6b**) presumably proceeds by an α-H elimination at Os, as was previously observed in the transformation

**Chart 2**

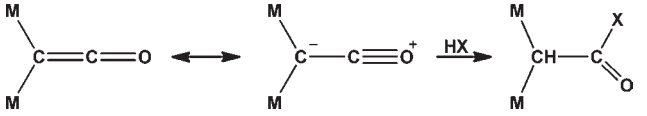


of the benzylidene unit in $[CpOsCl(P^iPr_3)(=C(Ph)H)]$ to a benzylidyne unit in $[CpOsH(P^iPr_3)(\equiv CPh)]^+$, initiated by chloride-ion removal.[30] α-H elimination at late metals is not common, so the observed transformation of **6a** to **6b** could also occur by a binuclear mechanism, in which oxidative addition of the Os-bound ketenyl-CH group at the adjacent Rh center is possible. However, this transformation seems less likely because it would lead to a Rh-bound hydride, which could not readily migrate to the observed site on Os owing to the intervening ketenylidene bridge. However, we cannot rule out prior migration of the ketenyl group to Rh followed by C−H activation by the adjacent Os; reversible migration of the ketenyl group from metal-to-metal, prior to oxidative addition, could be masked by the fluxionality described earlier.

Surprisingly few $\mu$-ketenylidene complexes are known. To our knowledge, the only late-metal examples are the poorly characterized, polymeric $[RhRh(CO)(C_2O)(COD)]_n$[31a] and binuclear $[Rh(acac)(CO)(C_2O)(COD)]_2$.[31b] Ketenylidene-bridged, early-metal complexes, $[M_3Cp_2(\mu_2\text{-}C_2O)(\mu_3\text{-}O)(O_2CN^iPr_2)_2]$ (M = Zr, Hf), are also known.[23a] Apparent examples of $\mu$-$C_2O$ complexes, $M_2C_2O$ (M = Ag,[32a] Au,[32b] Cu[32c]), in fact appear to have extended structures in which the ketenylidene ligands are symmetrically bridging *four* adjacent metals within two-dimensional sheets of the metals.[32a] These species remain poorly characterized; however, their reactivities support their proposed CCO bridges.[32a]

More commonly, ketenylidene ligands bridge three metal centers, for which two binding modes have been observed. The symmetric $\mu_3$ binding mode, in which the α-C symmetrically bridges the three metals,[25,33] can be viewed as a trimetallaacylium ion. In the second coordination mode, the ketenylidene group is tilted, symmetrically bridging a pair of adjacent metals (much like that observed in the work described herein) and, in addition, binding to a third metal in an $\eta^2$ manner via the C=C bond, as observed for $[(\mu\text{-H})_2Os_3(CO)_9(\mu\text{-CCO})]$,[20] formed by consecutive C−H bond activations and carbonyl insertion in $[Os_3(CO)_{10}(\mu\text{-CH}_2)(\mu\text{-CO})]$.[34] Similar reactivity has been observed with $[Ru_3(CO)_{10}(\mu\text{-CH})(\mu\text{-H})]$,[21] in which transformation to the ketenylidene/dihydride species, $[Ru_3(CO)_9(\mu\text{-H})_2(\mu\text{-CCO})]$, is proposed to occur via a ketenyl-bridged intermediate.[21]

In these previous examples, there was no evidence for the reversible conversion of ketenylidene/hydride species and ketenyl groups, as occurs in our case involving the tautomerism of **6a** to **6b**. For example, protonation of the dianionic species $[Ru_3(CO)_9(\mu\text{-CCO})]^{2-}$ occurs solely at the metals[22] to generate the dihydride-bridged, ketenylidene species noted above, leaving the ketenylidene group intact. Surprisingly, hydrogen migration to generate a ketenyl species did not occur in this case.

Transformation of the tautomeric mixture of **6a** and **6b** to give species **7a** in which a ketenyl-bridged group is also linked to dppm-H (see Scheme 5) is reminiscent of the reactivity of ketenes with protic acids (HX), which typically generates acid halides.[32] The resonance structures for the $\mu$-ketenylidene moiety, which can be considered as a dimetallaketene, shown


dx.doi.org/10.1021/ic102470j |*Inorg. Chem.* 2011, 50, 3523–3538

in Chart 2, offer a rationalization for the nucleophilicity of α-C. Protonation of the α-C of the ketenylidene-bridged species (**6b**) by the acidic dppm methylene group followed by nucleophilic attack by the deprotonated methanide C at the carbonyl C would generate the observed species **7a**, in which X is the methanide C of the deprotonated dppm group. Presumably, nucleophilic attack by the dppm methanide C occurs at a terminally bound ketenyl intermediate (much like that observed in **8**) for which rotation about the Os−ketenyl bond allows a trans arrangement of H and X, as observed in the product (**7a**).

## CONCLUSIONS

In this study, we have demonstrated the unusual behavior of both the NHC ligand, $IMe_4$, and the diphosphine, dppm. We find that inhibiting coordination of $IMe_4$ at a metal can instead initiate its Brønsted basicity, leading to ligand deprotonation. The deprotonated dppm (dppm-H) that is produced displays unusual chemistry. Interconversion between the more common $\mu$-$\kappa^1$:$\kappa^1$ binding mode of dppm-H, in which it binds through both phosphorus donors, and an unusual $\mu$-$\kappa^1$:$\eta^2$ mode, in which the methanide C of dppm-H additionally binds to one metal, is observed upon CO loss or addition, respectively. Furthermore, in the absence of CO, dissociation of the Rh-bound $PPh_2$ group of dppm-H occurs from $[RhOs(CO)_3(\mu\text{-}CH_2)(\mu\text{-}\kappa^1\text{:}\eta^2\text{-dppm-H})(dppm)]$, leading to coupling with the bridging methylene group to give a new bridging $Ph_2PCHP(Ph)_2CH_2$ ligand. In the presence of CO, proton transfer from the bridging $CH_2$ group to dppm-H occurs, accompanied by coupling of the transient methylidyne group with CO to give a ketenyl-bridged product and it ketenylidene-bridged hydride tautomer. This pair of tautomers is also unstable, converting slowly, by proton transfer from a dppm group to the ketenylidene moiety, leading to products in which the dppm-H methanide C is coupled to a metal-bridged ketenyl group.

## ASSOCIATED CONTENT

**Supporting Information.** Tables of crystallographic experimental details for compounds **3**, **5**, **6b**, **7a**, NMR spectra for compounds **3** and **6a**/**6b**, and atomic coordinates, interatomic distances and angles, anisotropic thermal parameters, and hydrogen parameters for compounds **3**, **5**, **6b**, and **7a** in CIF format. This material is available free of charge via the Internet at http://pubs.acs.org.

## AUTHOR INFORMATION

### Corresponding Author

*E-mail: martin.cowie@ualberta.ca. Fax: 01 7804928231. Tel.: 01 7804925581.

## ACKNOWLEDGMENT

We thank the Natural Sciences and Engineering Research Council of Canada (NSERC) and the University of Alberta for financial support for this research and the NSERC for funding for the Bruker PLATFORM/SMART 1000 CCD diffractometer, the Bruker D8/APEX II CCD diffractometer, and the Nicolet Avatar IR spectrometer. We thank the Department's Analytical and Instrumentation Laboratory and NMR Spectroscopy Laboratory for their outstanding support.

## REFERENCES

(1) (a) Wells, K. D.; McDonald, R.; Ferguson, M. J.; Cowie, M. *Organometallics* **2011,** 10.1021/om1010066. (b) Wells, K. D.; McDonald, R.; Cowie, M. *Organometallics* **2011**, *30*, 815.

(2) (a) Torkelson, J. R.; Oke, O.; Muritu, J.; McDonald, R.; Cowie, M. *Organometallics* **2000**, *19*, 854. (b) Sterenberg, B. T.; Hilts, R. W.; Moro, G.; McDonald, R.; Cowie, M. *J. Am. Chem. Soc.* **1995**, *117*, 245. (c) Brown, M. P.; Yavari, A.; Manojlovic-Muir, L.; Muir, K. W. *J. Organomet. Chem.* **1983**, *256*, C19. (d) Dominguez, R.; Lynch, T. J.; Wang, F. *J. Organomet. Chem.* **1988**, *338*, C7. (e) Camus, A.; Marsich, N.; Nardin, G.; Randaccio, L. *J. Organomet. Chem.* **1973**, *60*, C39. (f) Browning, J.; Bushnell, G. W.; Dixon, K. R. *J. Organomet. Chem.* **1980**, *198*, C11. (g) Briant, O. E.; Hall, K. P.; Mingos, D. M. P. *J. Organomet. Chem.* **1982**, *229*, C5. (h) Al-Jibori, S.; Shaw, B. L. *Inorg. Chim. Acta* **1983**, *74*, 235. (i) Hashimoto, H.; Nakamura, Y.; Okeya, S. *Inorg. Chim. Acta* **1986**, *122*, L9.

(3) (a) Ge, Y. W.; Sharp, P. R. *Organometallics* **1988**, *7*, 2234. (b) Ge, Y. W.; Sharp, P. R. *Inorg. Chem.* **1992**, *31*, 379. (c) Sharp, P. R.; Ge, Y. W. *J. Am. Chem. Soc.* **1987**, *109*, 3796. (d) Ye, C.; Sharp, P. R. *Inorg. Chem.* **1995**, *34*, 55. (e) Ge, Y. W.; Peng, F.; Sharp, P. R. *J. Am. Chem. Soc.* **1990**, *112*, 2632.

(4) (a) Kim, Y.-J.; Streitwieser, A. *J. Am. Chem. Soc.* **2002**, *124*, 5757. (b) Magill, A. M.; Cavell, K. J.; Yates, B. F. *J. Am. Chem. Soc.* **2004**, *126*, 8717. (c) Alder, R. W.; Allen, P. R.; Williams, S. J. *Chem. Commun.* **1995**, 1267. (d) Arduengo, A. J.; Calabrese, J. C.; Davidson, F.; Dias, H. V. R.; Goerlich, J. R.; Krafczyk, R.; Marshall, W. J.; Tamm, M.; Schmutzler, R. *Helv. Chim. Acta* **2009**, *92*, 2348.

(5) For examples, see: (a) Díez-González, S.; Marion, N.; Nolan, S. P. *Chem. Rev.* **2009**, *109*, 3612. (b) Cavallo, L.; Correa, A.; Costabile, C.; Jacobsen, H. *J. Organomet. Chem.* **2005**, *690*, 5407. (c) Dorta, R.; Stevens, E. D.; Scott, N. M.; Costabile, C.; Cavallo, L.; Hoff, C. D.; Nolan, S. P. *J. Am. Chem. Soc.* **2005**, *127*, 2485. (d) Jacobsen, H.; Correa, A.; Poater, A.; Costabile, C.; Cavallo, L. *Coord. Chem. Rev.* **2009**, *253*, 687. (e) Crabtree, R. H. *J. Organomet. Chem.* **2005**, *690*, 5451.

(6) For examples, see: (a) Grubbs, R. H. *Tetrahedron* **2004**, *60*, 7117. (b) Sanford, M. S.; Love, J. A.; Grubbs, R. H. *J. Am. Chem. Soc.* **2001**, *123*, 6543. (c) Sanford, M. S.; Ulman, M.; Grubbs, R. H. *J. Am. Chem. Soc.* **2001**, *123*, 749. (d) Dröge, T.; Glorius, F. *Angew. Chem., Int. Ed.* **2010**, *49*, 6940. (e) Lee, M.-T.; Lee, H. M.; Hu, C.-H. *Organometallics* **2007**, *26*, 1317.

(7) Kuhn, N.; Kratz, T. *Synthesis* **1993**, *6*, 561.

(8) Trepanier, S. J.; Dennett, J. N. L.; Sterenberg, B. T.; McDonald, R.; Cowie, M. *J. Am. Chem. Soc.* **2004**, *126*, 8046.

(9) Hilts, R. W.; Franchuk, R. A.; Cowie, M. *Organometallics* **1991**, *10*, 304.

(10) Programs for diffractometer operation, unit cell indexing, data collection, data reduction, and absorption correction were those supplied by Bruker.

(11) Beurskens, P. T.; Beurskens, G.; de Gelder, R.; Garcia-Granda, S.; Israel, R.; Gould, R. O.; Smits, J. M. M. *The DIRDIF-99 program system*; Crystallography Laboratory, University of Nijmegen: Nijmegen, The Netherlands, 1999.

(12) Beurskens, P. T.; Beurskens, G.; de Gelder, R.; Smits, J. M. M; Garcia-Granda, S.; Gould, R. O. *The DIRDIF-2008 program system*; Crystallography Laboratory, Radboud University Nijmegen: Nijmegen, The Netherlands, 2008.

(13) Altomare, A.; Burla, M. C.; Camalli, M.; Cascarano, G. L.; Giacovazzo, C.; Guagliardi, A.; Moliterni, A. G. G.; Polidori, G.; Spagna, R. *J. Appl. Crystallogr.* **1999**, *32*, 115–119.

(14) Sheldrick, G. M. *Acta Crystallogr.* **2008**, *A64*, 112–122.

(15) (a) Dawkins, G. M.; Green, M.; Jeffery, J. C.; Sambale, C.; Stone, F. G. A. *J. Chem. Soc., Chem. Commun.* **1980**, 1120. (b) Dawkins, G. M.; Green, M.; Jeffery, J. C.; Sambale, C.; Stone, F. G. A. *J. Chem. Soc., Dalton Trans.* **1983**, 499.

(16) Doherty, N. M.; Hogarth, G.; Knox, S. A. R.; Macpherson, K. A.; Melchior, F.; Morton, D. A. V.; Orpen, A. G. *Inorg. Chim. Acta* **1992**, *198*, 257.

(17) (a) Werner, H.; Schippel, O.; Wolf, J.; Schulz, M. *J. Organomet. Chem.* **1991**, *417*, 149. (b) Zurawinski, R.; Donnadieu, B.; Mikolajczyk, M.; Chauvin, R. J. *J. Organomet. Chem.* **2004**, *689*, 380. (c) Canac, Y.; Lepetit, C.; Abdalilah, M.; Duhayon, C.; Chauvin, R. *J. Am. Chem. Soc.* **2008**, *130*, 8406. (d) Hoover, J. F.; Stryker, J. M. *J. Am. Chem. Soc.* **1990**, *112*, 464.

(18) Sumner, C. E.; Collier, J. A.; Pettit, R. *Organometallics* **1982**, *1*, 1350.

(19) (a) Casey, C. P.; Marder, S. R.; Miles, W. H. *J. Mol. Catal.* **1983**, *21*, 173. (b) Casey, C. P.; Fagan, P. J.; Miles, W. H. *J. Am. Chem. Soc.* **1982**, *104*, 1134. (c) Casey, C. P.; Fagan, P. J.; Day, V. W. *J. Am. Chem. Soc.* **1982**, *104*, 7360. (d) Casey, C. P.; Gohdes, M. A.; Meszaros, M. W. *Organometallics* **1986**, *5*, 196. (e) Casey, C. P.; Woo, L. K.; Fagan, P. J.; Palermo, R. E.; Adams, B. R. *Organometallics* **1987**, *6*, 447.

(20) Shapley, J. R.; Strickland, D. S.; St. George, G. M.; Churchill, M. R.; Bueno, C. *Organometallics* **1983**, *2*, 185.

(21) Holmgren, J. S.; Shapley, J. R. *Organometallics* **1984**, *3*, 1322.

(22) Sailor, M. J.; Brock, C. P.; Shriver, D. F. *J. Am. Chem. Soc.* **1987**, *109*, 6015.

(23) (a) Calderazzo, F.; Englert, U.; Guarini, A.; Marchetti, F.; Pampaloni, G. *Chem.—Eur. J.* **1996**, *2*, 412. (b) McAllister, M.; Tidwell, T. *Can. J. Chem.* **1994**, *72*, 882.

(24) Moore, C. B.; Pimentel, G. C. *Chem. Phys.* **1963**, *38*, 2816.

(25) Kolis, J. W.; Holt, E. M.; Shriver, D. F. *J. Am. Chem. Soc.* **1983**, *105*, 7307.

(26) Uedelhoven, W.; Eberl, K.; Kreissl, F. R. *Chem. Ber* **1979**, *112*, 3376.

(27) Edwards, P. G.; Hahn, F. E.; Limon, M.; Newman, P. D.; Kariuki, B. M.; Stasch, A. *Dalton Trans.* **2009**, 5115.

(28) (a) van der Velden, J. W. A.; Bour, J. J.; Vollenbroek, F. A.; Beurskens, P. T.; Smits, J. M. M. *Chem. Commun.* **1979**, 1162. (b) Usón, R.; Laguna, A.; Laguna, M.; Manzano, B. R.; Jones, P. G.; Sheldrick, G. M. *J. Chem. Soc., Dalton Trans.* **1984**, 839. (c) Usón, R.; Laguna, A.; Laguna, M.; Gimeno, M. C.; Jones, P. G.; Fittschen, C.; Sheldrick, G. M. *Chem. Commun.* **1986**, 509. (d) Al-Resayes, S. L.; Hitchcock, P. B.; Nixon, J. F. *Chem. Commun.* **1986**, 1710. (e) Riera, V.; Ruiz, J. *Dalton Trans.* **1990**, 1607. (f) Fernández, E. J.; Gimeno, M. C.; Jones, P. G.; Laguna, A.; Laguna, M.; López-de-Luzuriaga, J. M. *Dalton Trans.* **1992**, 3365. (g) Fernandez, E. J.; Gimeno, M. C.; Jones, P. G.; Laguna, A.; Laguna, M.; Lopez-de-Luzuriaga, J. M. *Organometallics* **1995**, *14*, 2918. (h) Wiley, J. S.; Heinekey, D. M. *Inorg. Chem.* **2002**, *41*, 4961. (i) Langer, J.; Fabra, M. J.; García-Orduña, P.; Lahoz, F. J.; Oro, L. A. *Chem. Commun.* **2008**, 4822. (j) Gimbert, Y.; Lesage, D.; Milet, A.; Fournier, F.; Greene, A. E.; Tabet, J.-C. *Org. Lett.* **2003**, *5*, 4073. (k) Tejel, C.; Ciriano, M. A.; Jimenez, S.; Oro, L. A.; Graiff, C.; Tiripicchio, A. *Organometallics* **2005**, *24*, 1105. (l) Langer, J.; Wimmer, K.; Helmar, G.; Westerhausen, M. *Dalton Trans.* **2009**, 2951.

(29) (a) Tang, Y.; Sun, J.; Chen, J. *Organometallics* **1998**, *17*, 2945. (b) Tang, Y.; Sun, J.; Chen, J. *Organometallics* **2000**, *19*, 72.

(30) Esteruelas, M. A.; González, A. I.; López, A. M.; Oñate, E. *Organometallics* **2003**, *22*, 414.

(31) (a) Paiaro, G.; Pandolfo, L. *Angew. Chem., Int. Ed. Engl.* **1981**, *20*, 289. (b) Paiaro, G.; Pandolfo, L. *Gazz. Chim. Ital.* **1985**, *115*, 561.

(32) (a) Bryce-Smith, D.; Blues, E. T. *Chem. Commun.* **1970**, 699. (b) Bryce-Smith, D.; Blues, E. T. *Chem. Commun.* **1974**, 513. (c) Bryce-Smith, D.; Blues, E. T. *Chem. Commun.* **1973**, 921.

(33) (a) Hallgren, J. E.; Eschbach, C. S.; Seyferth, D. *J. Am. Chem. Soc.* **1972**, *94*, 2547. (b) Seyferth, D.; Hallgren, J. E.; Eschbach, C. S. *J. Am. Chem. Soc.* **1974**, *96*, 1730.

(34) Acre, A. J.; Deeming, A. J. *Chem. Commun.* **1982**, 364.